

*Biogeosciences*  
*Editorial board*

Lucerne, 15 June 2020

Dear Prof. Dr. Battin,

Thank you for the positive assessment of our manuscript “*Lake mixing regime selects apparent methane-oxidation kinetics of the methanotroph assemblage*” (bg-2019-482). On behalf of all authors, I am submitting a new version of the manuscript with the requested major revisions.

We implemented all major and minor comments of the three reviewers, as outlined previously in our author replies to the reviewer comments. I have included our final replies to the reviewer comments within this document. Further, we provide the marked-up version of the manuscript.

If there are further changes required, we are happy to hear from you.

Yours sincerely,

Magdalena Mayr

(On behalf of all authors: Magdalena J. Mayr, Matthias Zimmermann, Jason Dey, Bernhard Wehrli and Helmut Bürgmann)

*Major changes:*

We revised and improved Fig. 1 according to the reviewer comments by adding the measured temperature profiles. We also revised Fig. 3 according to the suggestions of reviewer 2 and 3. We now show an ordination in the main figure. Further, we provide taxonomic classification for the *pmoA* sequences (Fig. 3) as requested by reviewer 2 and 3 - and we also included a phylogenetic *pmoA* tree in the supplementary material (Supplementary Fig. 2).

In the revised manuscript we discuss in detail the relation between methane *affinity*, maximum methane oxidation rates, methanotroph biomass and their influence on the methane concentration in the epilimnion. To do so we provide the underlying rationale and calculations in the supplementary material. Further, we now discuss the influence of methane oxidation on the oxygen concentration in the epilimnion and provide an estimate.

Since there were several comments regarding the nature of the lake mixing regime and the characteristics of epi- and hypolimnion, we added a general paragraph describing the autumn overturn characteristics.

Further we added additional information to the methods section, as requested, and provide the custom databases used for finding *pmoABC* variants in the assembly as supplementary files.

## Reply to Reviewer 1:

The manuscript on "Lake mixing regime selects methane oxidation kinetics of the methanotroph assemblage" by Mayr and Zimmermann et al, is a well written manuscript on the ecophysiology of methanotrophic bacteria.

Answer: Thank you for the positive assessment.

I only have the following remarks: Method section on the kinetics: - As you describe in detail how you eliminated outliers from the calculations I was wondering what the percentage of outliers was? From my (more marine) experience it is difficult to get good kinetic data, as many of my "Kinetic incubations" only gave erratic results:

Answer: We show the elimination (in %) in the revised manuscript and further clarified the procedure and its motivation (also with regards to a comment by reviewer 2). See section 2.3.

Filtering the samples water on the 0.2  $\mu\text{m}$  filters. How long did it take to filter 1 – 2 liters on such a filter?? To my experience this may last very long: : . Thus, did you use any prefilters? And could the RNA composition change of this presumably longer time??

Answer: We did not record the exact duration but in our experience, filtration takes typically less than 10 and always less than 15 minutes. In order to retrieve enough RNA for metatranscriptomics and at the same time reducing filtration time as much as possible we used large (142 mm) diameter filters.

We did not use prefiltration since some filamentous methanotrophs can be quite large, with a length of up to >100  $\mu\text{m}$  (Oswald et al., 2017). We took the samples with a niskin bottle and we connected the tubing for the filtration device directly to the niskin bottle. The sample was kept shaded (inside the niskin bottle) and did not experience major temperature changes in the cool autumn/winter weather of the sampling season for this experiment. Thus, changes from the in-situ transcriptional profile are expected to be minor. In-situ filtration might still be preferable, but the equipment for this was not available to us at the time of this work.

We added the approximate time and the diameter of the filter to the revised manuscript as well as more details to clarify the steps that were taken to insure rapid preservation of the transcriptome. See section 2.7.

Result /Discussion - Figure 1: I think it is essential also to show the methane concentrations, in situ MOXrates and also the cell numbers in one figure, as the "environmental background information".

Answer: Methane concentrations were already shown in Fig. 1. We changed numbers with arrows to horizontal lines with numbers and units to increase clarity. We only measured methane at the sampling depths in this study. We show cell numbers and methane oxidation rates in Supplementary Figure 1.

The second part of fig. 1 the kinetics should go in a separate figure, as this is more an experimental aspect.

Answer: We used this format deliberately to directly connect the core (kinetic) data of the study with the graphs showing the environmental situation, which we hoped would make it easier for readers to understand how these are linked. We would therefore prefer to keep this format.

- Comment on figure 2: to me another way of seeing the data is, that in the epilimnion Km is much higher in October, but is getting more and more similar to the hypolimnion.

Answer: There might be a misunderstanding here. The epilimnion data are shown in orange, and thus are actually lowest in October. (See Fig. legend)

Thus it is not a mixing of two compartments but more of an approximation of the epilimnetic traits to the hypolimnetic ones ??

Answer: Indeed, as we show in a work that has in the meantime been published in *Communications Biology* (Mayr et al., 2020)(<https://doi.org/10.1038/s42003-020-0838-z>) there is more going on than simple mixing, i.e. complex dynamics of the community, and species mixed in from the hypolimnion typically do not establish in the mixed layer. This was also reflected in the transcriptomes obtained for this work. By the end of the mixing process however, almost the entire water mass was indeed mixed, and we observed only a small remnant of the hypolimnion. We did briefly outline our understanding of the dynamics in section 3.2 (L. 296-305) and added one paragraph on the general dynamics in seasonally stratified lakes, from stratification to fully mixed water column. There we also define how we use “epilimnion” and “hypolimnion” in the context of this study (Section 3.1, L. 239-253).

**References:**

Mayr, M. J., Zimmermann, M., Dey, J., Brand, A., Wehrli, B. and Bürgmann, H.: Growth and rapid succession of methanotrophs effectively limit methane release during lake overturn, *Commun. Biol.*, 3(1), 108, doi:10.1038/s42003-020-0838-z, 2020.

Oswald, K., Graf, J. S., Littmann, S., Tienken, D., Brand, A., Wehrli, B., Albertsen, M., Daims, H., Wagner, M., Kuypers, M. M. M., Schubert, C. J. and Milucka, J.: *Crenothrix* are major methane consumers in stratified lakes, *ISME J.*, 11(9), 2124–2140, doi:10.1038/ismej.2017.77, 2017.

## Reply to Reviewer 2:

Mayr, Zimmermann and colleagues studied the methane oxidation kinetics in the epilimnion and hypolimnion of a eutrophic lake during autumn/winter lake overturn and report changing methane uptake kinetics. Likewise, changes in pmoC, A and B gene expression profiles were observed, indicating adjustments in the active methanotrophic community in dependence on methane availability. I see value in the presented work, but also limitations and open questions that would have to be clarified.

Answer: Thank you for your valuable comments. In the following we answered and clarified all open questions and limitations raised.

First of all, I request the authors to point out that they measured apparent methane oxidation kinetics. This should be clearly indicated throughout the manuscript.

Answer: We changed to “apparent methane oxidation kinetics” in the title and throughout the text.

In this study, all conclusions are derived from 1 - 2 l of water per sample, taken at C1 four different time points of the epilimnion and hypolimnion, respectively. However, no replicate samples were taken per layer. I find this hardly acceptable. How representative are the findings of 1 l water for the whole stratification layer of a lake?

Can the authors be sure that the differences they see are indeed related to the respective water bodies? Already the molecular analysis of a second filter, which is a methodological replicate that was included for one sample, shows some differences (Fig. 3). Thus, I find it largely impossible to relate differences in the active methanotrophic community to stratification, especially in December and January and especially for pmoB and C (Fig. 3; statements l. 266-267), without knowing anything about the biological variation within a layer. The repeated measurements over time provide some evidence, but do not solve this issue when it comes to minor differences between specific samples.

Answer: Horizontal mixing in lakes is strong (Lerman and Chou, 1995, p. 86) especially in stratified lakes and horizontal variation within a lake (excluding near-shore water or parts with limited water exchange) is expected to be small (Yannarell and Triplett, 2004) in comparison with the vertical variation during stratification and temporal variation of the mixed layer. Taking one profile, usually close to the deepest point is therefore common practice for studies in smaller lakes or lake surveys (Oswald et al., 2017). Sample volume per depth is then typically decided by the requirements of the analytical methods rather than from concerns about the volume's representativeness.

In our earlier study on Rotsee we investigated the general population structure around the oxycline (Mayr et al., 2020a) and later the community composition change over time during lake overturn in considerable detail. We found that especially the mixed surface layer is a very homogeneous environment considering both environmental conditions and the methanotroph assemblage (Mayr et al., 2020b). Therefore, we think that the epilimnion measurements are indeed representative for the mixed layer (epilimnion in this study) and only very small variabilities would be expected from multiple measurements. The focus of this study was not on variability within the mixed layer or within the hypolimnion, but rather to demonstrate that differences in kinetic parameters occur at all, in contrasting microbial communities within one lake which has not been demonstrated before. Therefore, although we did not study the variation within a layer in this study, we had considerable previous knowledge on the same lake from the years before and designed the study on this basis.

The hypolimnion during stratification by definition shows very different conditions to the epilimnion, but gradients of methane and other parameters can be observed within the hypolimnion. Therefore, whereas the hypolimnion is less homogeneous than the epilimnion, the difference to the epilimnion is clear, based on both, the environmental conditions (orders of magnitude higher methane concentrations) and a different methanotrophic assemblage (this study and Mayr et al., 2020b, 2020a).

Regarding the request for (biological) replication of the kinetic measurements, we have to note that, although measuring different depths and or replicates from the layers would be favourable, we had to adjust the amount of incubations to our handling limit of the required incubations. We decided to improve the replication for the respective depths to have enough data points to determine the affinity of the respective depth (see our answer on outlier elimination to the other reviewer). Thus, in order to have enough different methane concentrations and technical replication we could only analyse two depths. This decision was also based on the results obtained in our previous study of the lake overturn period as discussed above (Mayr et al., 2020b). Therefore, we could not have analysed more replicates or depths on one date due to practical limitations on the number of incubations that we could handle, but we believe that the multiple time points provide confidence in our measurement. The reviewer may note that the existing studies on apparent MO kinetics in lakes were indeed all done on lower numbers of samples.

We agree that the difference between epi- and hypolimnion become smaller in December and January, which is expected as the epilimnion is increasing in size and stratification of the lake weakens. In January the hypolimnion is almost gone and only small differences remain between epi- and hypolimnion, both in terms of methane concentration and methanotroph composition. We agree that the characteristics of the epi- and hypolimnion change over time (which is expected and was part of our research question) and use the terms epi- and hypolimnion more to clarify where the sample was taken, rather than to imply homogeneity within the category. Because there is a temporal variation, we also do not give average values for the epi- or hypolimnion. We agree that the term hypolimnion for the bottom sample in January might be misleading without further information, because the lake has almost completely mixed, and the strong difference seen between epi- and hypolimnion before are no longer present.

In the revised manuscript we added one paragraph on the general dynamics in seasonally stratified lakes (L. 239ff), from stratification, lake mixing and the fully mixed water column to section 3.1. Further, we explain within this paragraph and the following the characteristics of epi- and hypolimnion and how we use “epilimnion” and “hypolimnion” in the context of this study, and include some information on our previous study (Mayr et al., 2020b; Zimmermann et al., 2019) on which we based the present study.

Besides, the reason for including one experimental replicate (January, hypolimnion) or the conclusions derived from this sample are not mentioned anywhere.

Answer: We included this replication in order to increase confidence in the transcriptomic analysis. It is not easy to obtain enough RNA for metatranscriptomics from our lake samples, which we tried to optimize as much as possible considering the trade-off between 1) filtration time and 2) obtaining enough sample for RNA extraction and subsequent sequencing. Because both effort and costs are high, we included only one replicate, although we of course agree more would be favourable. Typically, RNA-based measurements show a somewhat larger variability than DNA-based sequencing results, therefore we think that our replicate shows that the results are very reproducible for a metatranscriptomic analysis, but the result also cautions that small differences between samples should not be overemphasized. That all three January samples are basically indistinguishable based on metatranscriptomics is not surprising as the mixing process is almost complete in January and the conditions at the sampled depths are very similar at this date (see answer above).

We added a short explanation to the revised manuscript (Methods section 2.7, L. 184) and also added conclusions derived from this sample to the revised manuscript (Results and Discussion, section 3.3, L. 412).

How do the authors know that they had a representative sample from the hypolimnion at the last sampling date? There is no change in temperature evident and the decline in oxygen concentrations does not reach oxygen concentrations as low as at the earlier time points. Likewise, methane concentration in this sample is not as high as in the other samples from the hypolimnion. Thus, it appears that the sample was not taken at appropriate depth to be comparable with the others.

Answer: During lake overturn the mixed layer (corresponding to epilimnion in our study) increases over time due to gradual cooling and the resulting density change. By January this mixing process is almost complete and the conditions in the remaining “hypolimnion” differ from those earlier in the season. However, the water at the lake bottom at the time of sampling still showed a small differences of e.g. methane and oxygen concentration to the water above, although the temperature gradient is gone (Figure 1d). The lake has a max. depth of 16 m and our sample was taken from 15 m, the maximum depth that can be sampled with the niskin bottle without disturbing the sediment. Therefore, if the sample in January is truly a “hypolimnion” sample is indeed somewhat debatable but refers to the bottom location of the sample as for the other sampling dates.

In the revised manuscript we added one paragraph on the general dynamics in seasonally stratified lakes and defined our use of epi- and hypolimnion more clearly (see answer above).

The conclusion about the specific enrichment of well-adapted methanotrophs with particular methane oxidation kinetics (L. 23) is conceivable, but should be drawn more carefully, because it remains unclear whether the observed kinetics are indeed adaptations of particular competitive methanotrophs under oligotrophic conditions, especially with regard to affinity. As only apparent parameters could be estimated, it remains unclear whether the methane monooxygenase of the respective organisms has indeed a higher affinity (lower  $K_m$ ) and is thus more competitive. It should be kept in mind in this context that a low apparent  $K_m$  is not necessarily a specific adaptation to low methane concentrations, but can be the result of starvation (see Dunfield and Conrad 2000, AEM).

Answer: It is of course true that we only measured the apparent kinetic properties of the whole MOB assemblage. Our conclusion is based on the observation that changes in the apparent kinetic properties of the assemblage are accompanied by changes in the community composition and changes in the expression level of *pmoCAB* variants of the assemblage. In this respect, we draw conclusions on an average trend on the community level but we are well aware that there might be additional mechanisms, e.g. on individual species level as well.

In the revised manuscript we stated (L. 24) more carefully *as one* important factor for creating niches. Further, we discussed (L. 307-311 Results and Discussion section) the additional explanation, that changes in  $K_m$  can be a result of starvation (Dunfield and Conrad, 2000). We also note that Dunfield and Conrad (2000) observed a constant specific affinity ( $a_0$ ), which is in contrast to our results. In our case both  $K_m$  and  $a_0$  change with depth and with time, which suggests adaptation rather than starvation as described in Dunfield and Conrad (2000).

Whether the kinetic differences, assuming they have a genetic basis, have an influence on the competitiveness of a species is indeed a very interesting question. We are currently preparing a manuscript that discusses a modelling approach in which we investigate the interplay of MOB populations consisting of “species” with varying  $K_m$  and  $V_{max}$  and their competitiveness in the Rotsee setting in detail.

To determine methane uptake kinetics (Fig. 2), the samples were apparently incubated at the temperatures measured in the epilimnion. However, samples from the hypolimnion encounter much lower temperatures in autumn. How does that affect comparability of the obtained results and conclusions about in situ conditions? This should be taken into account.

Answer: We clarified the rationale for our approach in the methods section 2.3 (L. 118-120) and mention the caveats that arise from this choice. Our approach was not designed to obtain the most realistic in-situ rates, but to get a valid comparison of the apparent kinetics in the different communities of the sampled water layers. To be able to compare the measured kinetics between epi- and hypolimnion at each given date, we measured them at the same temperature, since temperature influences the solubility of gases (methane).

Related to this point: Considering that altered temperature and oxygen conditions were used to characterize the methane uptake kinetics in vitro, to what extent can the findings be translated to in situ conditions, considering that these factors can affect the measured  $K_m$  and  $V_{max}$  (see the study of Thottathil et al 2019, who report that increasing oxygen concentrations in lake water can reduce maximum methane oxidation rates;

doi.org/10.1007/s10533-019-00552-x). Is it conceivable that  $V_{max}$  in the hypolimnion is underestimated when determining oxidation rates at higher oxygen concentrations in vitro?

Answer: Our main goal was to compare apparent kinetics as a trait of microbial communities rather than to obtain precise information on in-situ kinetics. In an attempt to measure methane affinities under as standardized conditions as possible we measured the methane oxidation kinetics under similar conditions to the best of our knowledge. We added this rationale behind the methane affinity experiments to the methods section. Further, we add that altered temperature and oxygen concentration as compared to the in-situ conditions may influence the result as a limitation of our study to the discussion section (L. 291-295).

I find it very unfortunate that the identification of methanotrophs stops at the level “type Ia, type Ib, type II”. The sequence information should provide more detailed information about the identity of the methanotrophs. At least for *pmoA* comprehensive datasets are available covering besides cultivated strains diverse groups of uncultivated taxa, so that more information could have been extracted here to identify conspicuous taxa.

Answer: In the revised manuscript we provided an improved classification of *pmoA* based on the NCBI refseq\_protein database and a *pmoA*-based phylogenetic tree (Supplementary Figure 2) of the sequences found in this study and reference sequences. The taxonomic affiliations were also added to Figure 3 and Supplementary Figure 3. We note that the *pmoABC* sequences are available as fasta files via our data repository.

Specific comments: l. 19 and 291: According to the data in table S1, the difference in  $K_m$  is 20-fold, not 2 orders of magnitude

Answer: That’s correct, we have corrected this.

l. 25: Where in the presented work is it shown or discussed that 90% of the methane are removed? It appears that this is not a conclusion that is derived from the presented work.

Answer: This is a result from our work on the overturn of the same lake one year prior to the present study (Zimmermann et al., 2019), and is based on using mass balance analysis and modelling. We provided a clear reference for the statement in question in the revision (L. 41-44) and rephrased the sentence in the Abstract.

l. 65: Metagenomic data were used as a basis for the metatranscriptomic data analysis, but are not presented independently; thus, I would not emphasize the metagenomics approach here for the analysis of MOB assemblages.

Answer: We deemphasized the metagenomics part here.

l. 73: Five campaigns in autumn 2017 does not appear correct (three samplings in 2017 and one in 2018 according to the presented results)

Answer: Yes, we have changed this accordingly.

l. 74-75: More measured parameters are given here than presented; harmonize.

Answer: We harmonized the methods part accordingly in the revised manuscript.

l. 78: I do not find any helpful information about the radio isotope tracer technique in Steinle et al 2015. While the cited references enabled me to understand how methane oxidation rates were determined, they do not allow me to evaluate whether/how this procedure can be used to survey methane oxidation kinetics.

Answer: We improved the methods section and added reference to Lofton et al. (2014) who derived methane oxidation kinetics from methane oxidation rates that were measured using  $^{14}\text{C-CH}_4$ . As described in Busmann et al. (2015), the  $^3\text{H-CH}_4$  tracer technique is more sensitive than the  $^{14}\text{C-CH}_4$  technique and therefore allows shorter incubation times and rate determination at low  $\text{CH}_4$  concentrations. The combination of the approaches is a novelty of our work.

l. 80: How much methane was in this mixture?

Answer: We specified the amount of methane in the mixture in the methods section. L. 93-95 “The specific activity of  $^3\text{H-CH}_4$  is  $0.74 \text{ TBq mmol}^{-1}$  and the  $200 \mu\text{L}$  of gaseous  $^3\text{H-CH}_4/\text{N}_2$  mixture therefore contained  $108 \text{ pmol } ^3\text{H-CH}_4$ . In comparison, the  $500 \mu\text{L}$  gas bubble with the lowest concentration of unlabelled methane, contained  $17 \text{ nmol CH}_4$ .”

l. 100-106: The authors describe different criteria that were used to identify and eliminate outliers here. Point four states that data points were removed in case less than two replicates remained. According to l. 93, duplicates were prepared. Does that mean that data for a specific methane concentration were lost each time one of the two replicates was identified as outlier? In this context, it is also unclear what Fig. 1 e-h shows. Do the presented data points represent individual measurements or are these mean values of the two replicates? Sometimes, I see two data points at a specific concentration, but sometimes I see only one point. Please clarify.

Answer: In a revised manuscript we have improved clarity and the level of detail in the methods section 2.,3 L127+.

It would be valuable to know how many high-quality reads the authors generated per sample in the metagenomic and metatranscriptomic analysis, respectively.

Answer: For metagenomics we generated approx. 31-37 million reads and for metatranscriptomics 26.6 – 34 million reads. We provided this information in the methods section of the revised manuscript. Section 2.7, paragraph 2.

l. 157: Why three samples in October; to my understanding there should be one from the epilimnion and one from the hypolimnion per point of time.

Answer: We measured one additional depth in October in between epi- and hypolimnion, which is included in the data repository but is currently not discussed in the manuscript. We did not pursue the intermediate sample in later campaigns since we concluded that focusing our effort on the Epilimnion and Hypolimnion (e.g. continuing with measurement triplicates) would be better. We did however use the metagenomics data from this sample to improve the assembly. We stick to the two-depth presentation for the main manuscript and figures as it keeps the story focused. However, we added the information on this additional sample in the methods section (Metagenomic and metatranscriptome analysis, 2.7, L. 203-205).

l. 163: Can a few words be added to describe this custom database? How was it set up? What type of data does it include?

Answer: We prepared three custom databases, one for each gene: *pmoA*-like, *pmoB*-like, *pmoC*-like. We extracted *pxmABC*, *pmoCAB2*, *pmoCAB* from both alpha- and gamma-proteobacterial genomes manually. Note that *pmoCAB2* is only known from alphaproteobacterial methanotrophs as yet. We used amino acid sequences with diamond blastp to find the genes in our metagenome and transcriptome. The custom database was especially important for *pmoC* which was not included in the available prokka databases. A short description was added to the revised manuscript (section 2.7, L. 213-215), and the databases were added as supplementary files 1-3.

l. 202-205, l. 295 and perhaps elsewhere: wording: do the authors refer to  $K_m$  or  $a_0$  here when talking about affinity?

Answer: We refer to  $1/K_m$  when talking about *affinity* (L. 106). We refer to  $a^0$  (L. 141) when we talk about *specific affinity* (defined as the ratio  $V_{max}/K_M$ ). We made sure that these terms are clearly defined on first use and put the kinetic parameter terms in italics throughout to help to distinguish them in the text.

l. 204-207: I cannot follow argumentation here. And how do the authors explain that the organisms with the higher  $V_{max}$  and lower  $K_m$  disappear in January (Fig. 1h), although they should have a competitive advantage?

Answer: The fact that certain types disappear when they should have a competitive advantage with respect to the methane oxidation kinetics (at least insofar as we can conclude on the traits of individual species from the measurements performed on consortia) indeed leads us to the conclusion that one would need to consider additional traits to explain the observed abundance pattern and its dynamics. As stated on L. 290-302 we believe that there have to be additional important differences in other traits (i.e. temperature optimum or specific adaptations to low or high oxygen concentrations). We already have strong indications from our previous work that these factors are indeed important (Mayr et al., 2020a, 2020b). Nonetheless, we do observe significant differences and changes in the methane oxidation kinetics which are related to the differences and changes in the environment. We have incorporated the information above in sections 3.2 (L301-305) and 3.3 (L. 407-4017) of the revised manuscript.

l. 241: A range of 1 – 40 is a bit outdated. Atmospheric methane oxidizers in soil are meanwhile known to have  $a_0$ s values with up to  $195 \times 10^{-12}$  L/cell\*h (Tveit et al) and in upland soils, estimates are ranging up to  $800 \times 10^{-12}$  L/cell\*h (Kolb et al 2005; doi:10.1111/j.1462-2920.2005.00791.x)

Answer: Thank you, we updated this.

l. 248-250: I find the 25% and 93% values critical here, because huge differences are observed at the individual time points. Especially the 93% value appears to be strongly affected by the huge difference observed in December.

Answer: We have now formulated a more differentiated argument: Individual percentages can be calculated from the individual values for the maximum methane oxidation rate as well as the in-situ methane oxidation rate in Supplementary Table 1. In the epilimnion there might indeed be a trend over time, however all values are below 50%. In the hypolimnion we observe less variation and all values are above 67%. Therefore, we do believe that it is a valid conclusion that MOB in the epilimnion were generally more limited than MOB in the hypolimnion.

l. 254: What do the authors mean with aggregate properties here? What aggregates do they refer to?

Answer: “Thus, the reported kinetics reflect aggregate properties of the respective assemblage.” Aggregate was used in the sense of “formed or calculated by the combination of several separate elements”, in this case of all the species and individuals in the community, i.e. we meant to express that the reported kinetics reflect the (apparent) properties of the MOB assemblage which is present at the depth and date of sampling. In the revised manuscript we change the term to “composite”.

l. 256 – 258: It would be very valuable if the described findings could be seen in Figure 3.

Answer: We rearranged Figure 3 according to the remarks of reviewers 2 and 3 to better visualize the changes in the transcriptionally active methanotroph assemblage.

We calculated a correspondence analysis (cca, vegan) instead of the detrended correspondence analysis (decorana, vegan) (detrending was not necessary, because no arch effect was visible) because the more common scaling option 2 is not implemented in decorana. Further, we made the taxonomic affiliations visible with a color code in

the ordination (Fig. 3a) and added taxonomic information to the legend for Fig. 3b. To save space and because similar information is shown in the analogous figures for *pmoB* and *pmoC*, we moved them to the Supplementary Material (Supplementary Fig. 3a-d) including taxonomic information in the legend.

l. 292-293: The transcription of genes does not relate to enzyme affinity or apparent Km values; thus, I cannot follow argumentation here.

Answer: The association is only correlational so far, this is true. We clearly stated this as a hypothesis in the revised manuscript (L. 429).

l. 301: I do not necessarily agree to the term “entirely” in the context with “kinetic traits”; other environmental conditions may have affected the kinetic parameters. Please keep in mind that you can only measure apparent parameters, not enzyme kinetics.

Answer: We have removed the “entirely” there (L. 440). Yes, it is true that other parameters likely influence kinetic traits. We keep in mind that we do not measure enzyme kinetics but apparent kinetics. Nevertheless, our metatranscriptomics data clearly suggest that pMMO was by far the most expressed methane oxidizing enzyme. Therefore, according to our data most of the methane which is oxidized is oxidized by pMMO and not other enzymes.

l. 303-304: Please note that *Methylocapsa gorgona* does not possess a second *pmoA* gene for “high-affinity oxidation” despite being able to live on very low methane concentrations (Tveit et al).

Answer: Yes, we are aware of this interesting study and cite it elsewhere in the manuscript. *Methylocapsa gorgona* can live and grow on very low methane concentrations, but it does not have a very low apparent Km (4.9  $\mu$ M), but it has a very high specific affinity. But many methanotrophs possess sMMO and pMMO, and sMMO has a lower affinity than pMMO. To our knowledge *Methylocapsa gorgona* does not have sMMO.

References: The reference list does not allow to differentiate publications (e.g. Mayr et al 2019a, b, c). The reference list lacks information about the year the work has been published and the indices a,b,c.

Answer: Here we followed the author guidelines of the Journal and added the year + a,b,c at the end of the reference. The year changed in two cases.

Mayr, M. J., Zimmermann, M., Dey, J., Wehrli, B. and Bürgmann, H.: Data for: Community methane-oxidation kinetics selected by lake mixing regime [Data set], Eawag Swiss Fed. Inst. Aquat. Sci. Technol., doi:10.25678/0001fa, **2019**.

Mayr, M. J., Zimmermann, M., Guggenheim, C., Brand, A. and Bürgmann, H.: Niche partitioning of methane-oxidizing bacteria along the oxygen–methane counter gradient of stratified lakes, ISME J., 14(1), 274–287, doi:10.1038/s41396-019-0515-8, **2020a**.

Mayr, M. J., Zimmermann, M., Dey, J., Brand, A., Wehrli, B. and Bürgmann, H.: Growth and rapid succession of methanotrophs effectively limit methane release during lake overturn, Commun. Biol., 3(1), 108, doi:10.1038/s42003-020-0838-z, **2020b**.

Figure 1: The axis showing oxygen concentrations should have a more increments.

Answer: We provide more increments on the oxygen axes in the revised Fig. 1.

Figure 2: explain error bars

Answer: We improved clarity of the caption of Fig. 2.

Figure 3: The distinction by color is difficult in plots a1-c1; why not choosing more distinct colors / a broader range of colors per plot? This is of particular importance, as the relative abundances cannot be taken from Table S2 without additional calculations. It is currently impossible to identify type Ib or type II methanotrophs based on the color code and without further invest. However, as pointed out above, it would be even more valuable if more taxonomic information could be provided.

Answer: Thanks for the valuable suggestions for Figure 3. Unfortunately, we could not find a better and still colour-blind proof color palette. We decided that taking a clear brightness-based palette with additional colour information would be best. As described above we made general improvements to the data visualization of Fig. 3 based on the comments of reviewer 2 and 3 by improving the ordination-visualization and moving it to the main text. Further, we added improved taxonomic information to the legend and provide a *pmoA* phylogenetic tree in the supplementary material. Further, we provide the supplementary table with the underlying data as a tab delimited file instead of a pdf to make it more accessible. The fasta files of all *pmoABC* variants are available in the provided data repositories (“Data availability”).

Table S3: Provide reference for Knief et al 2015.

Answer: We provided the reference in the revised manuscript.

#### References:

- Bussmann, I., Matousu, A., Osudar, R. and Mau, S.: Assessment of the radio  $^3\text{H-CH}_4$  tracer technique to measure aerobic methane oxidation in the water column, *Limnol. Oceanogr. Methods*, 13(6), 312–327, doi:10.1002/lom3.10027, 2015.
- Dunfield, P. F. and Conrad, R.: Starvation alters the apparent half-saturation constant for methane in the type II methanotroph *Methylocystis* strain LR1, *Appl. Environ. Microbiol.*, 66(9), 4136–4138, doi:10.1128/AEM.66.9.4136-4138.2000, 2000.
- Lerman, A. and Chou, L.: *Physics and chemistry of lakes*, [Second ed., Berlin [etc.] : Springer-Verlag., 1995.
- Lofton, D. D., Whalen, S. C. and Hershey, A. E.: Effect of temperature on methane dynamics and evaluation of methane oxidation kinetics in shallow Arctic Alaskan lakes, *Hydrobiologia*, 721(1), 209–222, doi:10.1007/s10750-013-1663-x, 2014.
- Mayr, M. J., Zimmermann, M., Guggenheim, C., Brand, A. and Bürgmann, H.: Niche partitioning of methane-oxidizing bacteria along the oxygen–methane counter gradient of stratified lakes, *ISME J.*, 14(1), 274–287, doi:10.1038/s41396-019-0515-8, 2020a.
- Mayr, M. J., Zimmermann, M., Dey, J., Brand, A., Wehrli, B. and Bürgmann, H.: Growth and rapid succession of methanotrophs effectively limit methane release during lake overturn, *Commun. Biol.*, 3(1), 108, doi:10.1038/s42003-020-0838-z, 2020b.
- Oswald, K., Graf, J. S., Littmann, S., Tienken, D., Brand, A., Wehrli, B., Albertsen, M., Daims, H., Wagner, M., Kuypers, M. M. M., Schubert, C. J. and Milucka, J.: *Crenothrix* are major methane consumers in stratified lakes, *ISME J.*, 11(9), 2124–2140, doi:10.1038/ismej.2017.77, 2017.
- Yannarell, A. C. and Triplett, E. W.: Within- and between-Lake Variability in the Composition of Bacterioplankton Communities: Investigations Using Multiple Spatial Scales, *Appl. Environ. Microbiol.*, 70(1), 214–223, doi:10.1128/AEM.70.1.214-223.2004, 2004.
- Zimmermann, M., Mayr, M. J., Bouffard, D., Eugster, W., Steinsberger, T., Wehrli, B., Brand, A. and Bürgmann, H.: Lake overturn as a key driver for methane oxidation, *bioRxiv*, doi:10.1101/689182, 2019.

### Reply to Reviewer 3:

This manuscript describes the study of methane oxidation (MOX) during lake overturn in Lake Rotsee in Switzerland. You combine measurements of MOX kinetics with metatranscriptomic analyses of methane monooxygenase genes and report differences between epi- and hypolimnion during stratification and a convergence of MOX kinetics and gene expression during lake water mixing. You conclude that methane oxidizers with well-adapted kinetics occupy distinct niches in stratified lakes.

Answer: Thank you for your valuable comments. In the following, we address all open questions and limitations raised.

While I think the report of kinetic parameter of methane oxidation is of great relevance, however, I found that the manuscript suffers from a lack of clarity and over-simplifications. Most importantly, it's unclear how the central conclusion, that well-adapted methanotrophs inhabit niches depending on methane availability (in hypo- and epilimnion), is reached. Wouldn't a match between in situ CH<sub>4</sub> concentration and K<sub>m</sub> (not normalized per cell) be a stronger indication of such an adaptation?

Answer: Thank you for your positive assessment of the relevance of reporting kinetic parameters. We improved the clarity of our central conclusion and added a steady state calculation to show how K<sub>m</sub> values and in-situ methane concentrations are linked to the supplementary material "Supplementary Calculation". Further we discuss this calculation in the main text in L. 329-338:

"We thus concluded that MOB assemblages displayed a specific adaptation to the prevailing methane concentrations based on the fact that we observed a higher *affinity* (low K<sub>m</sub>) in the low-methane epilimnion compared to the methane rich hypolimnion as long as stratification is present. That the K<sub>m</sub> values of the assemblage in the epilimnion do not match the *in-situ* methane concentrations is not unexpected: In the mixed layer and under the assumption of a steady-state, the flux of methane from the hypolimnion is balanced by the methane oxidation rate. Under these conditions, the *in-situ* methane concentration depends on the half-saturation constant (K<sub>m</sub>) but should be lower than it (Supplementary Calculation 1). Per definition, the half-saturation constant is the substrate concentration where the growth rate is half the maximum growth rate. Even if the growth rate is only half the maximum growth rate, microbial methane oxidation continues, and methane concentrations decrease to values below K<sub>m</sub>."

I also believe a better use of the metatranscriptomic data could help to strengthen this point. A finer taxonomic resolution based on the *pmoCAB* genes and a more quantitative characterization of the community turnover should be possible – and could help to make the point that indeed there are distinct populations of MOB that are adapted to in situ CH<sub>4</sub> concentration. Accordingly, I think that Figure 3 a1-c1 is not the ideal way to convey this important point. Maybe a combination of SI Fig. 2 (which I think shows quite nicely the convergence towards similar gene expression patterns in January, with a Figure showing the taxonomic composition of MOB during lake overturn would be a better choice.

Answer: Yes, we agree.

We provided a finer taxonomic resolution for *pmoA* in the revised manuscript. We now provide a phylogenetic tree in Supplementary Figure 2 and added this classification to Figure 3a and b, as well as Supplementary Figure 3a, b. *pmoC* and *pmoB* are less indicative for taxonomic classification because they are not as frequently sequenced and used for this purpose. Therefore, we only classified them to family level and used the same finer taxonomic resolution if a respective sequence was found on the same contig with a taxonomically classified *pmoA*. The full list is provided as .txt file (Supplementary file 4). We note that the *pmoABC* sequences are available as fasta files via our data repository.

Thanks for the suggestion regarding Figure 3. We rearranged Figure 3 according to the remarks of Reviewer 2 and 3 to better visualize the changes in the transcriptionally active methanotroph assemblage.

We calculated a correspondence analysis (cca, vegan) instead of the detrended correspondence analysis (decorana, vegan) (detrending was not necessary, because no arch effect was visible) because the more common scaling option 2 is not implemented in decorana. Further, we made the taxonomic affiliations visible with a color code in the ordination (Fig. 3a) and added taxonomic information to the legend for Fig. 3b. To save space and because similar information is shown in the analogous figures for *pmoB* and *pmoC*, we moved them to the Supplementary Material (Supplementary Fig. 3a-d) including taxonomic information in the legend.

Moreover, I was somewhat irritated by the rather vague description of the environmental conditions during lake overturn. The traditional definition of lake stratification and hence the difference between epi- and hypolimnion based on temperature rather than oxygen. And while the manuscript addresses MOX during lake overturn, you refer to the oxycline for sampling. I understand that the temperature profiles shown in SI Fig 1 may not be as clear as the oxygen profiles shown in Fig. 1 – but I would advise to show all profiles (also conductivity which should explain the inverse stratification pattern in December) and to be very clear with the definition of overturn, thermos- and oxycline.

Answer : We added temperature profiles to Figure 1 and used the terms overturn, thermo- and oxycline more carefully.

Finally, given the relatively low number of samples and the fact that the pattern was (only) observed in Lake Rotsee, I think the manuscript should be thoroughly rewritten to make clear that this may reflect a specific situation in the (relatively eutrophic) Lake Rotsee. Also, there are several cases of speculation or exaggerated extrapolation, which should be avoided.

Answer: The effort of obtaining the time resolved data for two water layers was very substantial (described in the answers to Reviewer 1 and 2). Nevertheless, we agree that we only have a limited number of samples from a single lake. We highlighted this more clearly and explicitly stated that further investigations in other lakes will be required to confirm our findings.

L 11 In freshwater lakes... so, this excludes saline lakes? Consider removing “freshwater”

Answer: We removed freshwater here and mention it in Line 14: “in a seasonally stratified freshwater lake”.

L 14 we tested the hypothesis that methanotroph assemblages in a seasonally stratified lake...

Answer: We changed this accordingly and toned down the conclusions in order to avoid overselling.

L 18 consider a brief explanation of the meaning “half-saturation constant” here

Answer: We added a brief definition of „half-saturation constant“ (L. 19-20).

L19 ...Km differed by two orders of magnitude – but in the results it seems that they differed between 15 and 0.7 uM (a factor of ~20)

Answer: We corrected this.

L 25 ...90% of what?

Answer: 90% of the methane that is transferred to the epilimnion during lake overturn is oxidized. Since this is a result from an earlier study we rephrased the sentence (L.43-44).

L28 can you talk about a climate IMPACT of lacustrine systems?

Answer: Yes, we think so. According to DelSontro et al. (2018), lacustrine systems emit an equivalent of about 20% of the global fossil fuel CO<sub>2</sub> emissions, and methane contributes approx. 75% to this. Continuing eutrophication of lacustrine systems will most likely further increase emissions by another 30-90% (Beaulieu et al., 2019; DelSontro et al., 2018). We clarified: “Methane is a major contributor to the climate impact of the greenhouse gas emissions from lakes”.

L 31 anoxic habitats.... In the oxygen-depleted hypolimnion... repetitive

Answer: We removed “anoxic habitats” in the revised manuscript.

L 47 kinetic traits... Use kinetic parameter instead (see L 48)

Answer MZ: We have harmonized the use of “kinetic traits” and “kinetic parameter” in the revised manuscript.

L 58 ...Lake Rotsee...

Answer: We removed the “a” written before “Lake Rotsee”.

L 63 ex situ consider replacing with “laboratory incubations”

Answer: We replaced this as proposed (L. 71)

L 73 four or five campaigns?

Answer: We corrected this to four campaigns.

L 77 and onward. Please provide more detail on this method including how the killed controls were treated.

Answer: We provided more detail on how the killed controls were treated (section 2.3, L.110-116).

L 91 how were Schott bottles sealed air-tight?

Answer: The Schott bottles were not sealed air-tight. Since gasses were stripped from the samples anyway for these analyses, this was not necessary. For determinations of methane concentration and “in-situ” rates, we directly filled samples into serum vials and those were sealed air-tight (see sections 2.4, 2.5).

L 110 we determined the in-situ MOX rate... in duplicate ex-situ incubations... Confusing, please rewrite.

Answer: We removed “in-situ” and changed ex-situ incubations to laboratory incubations throughout the manuscript.

L 161 an 167 reads shorter than 400 or 300 bp were removed?

Answer: We first used a general approach to identify genes (prodigal) removing <400bp genes. During targeted gene identification with prokka and diamond again shorter gene pieces of MMO were identified and we removed short gene fragments <300bp in the original manuscript. In the revised manuscript we harmonized this and used 400bp base pairs as a cut-off in both steps.

L 183 aerobic methane oxidation likely contributed to this oxygen depletion in the epilimnion. This seems very speculative for me. Could a back of the envelope calculation, e.g. knowing the volume and CH<sub>4</sub> concentration in the hypolimnion and the stoichiometry of MOX be used to support this speculation?

Answer: We added a short calculation to the main text that supports that methane oxidation substantially contributed to the oxygen depletion. (Section 3.1, L.261-278)

“The oxygen concentration shifted from 15% oversaturation in October to 67% undersaturation in December (Fig. 1a-d), aerobic methane oxidation likely contributed to the oxygen depletion in the epilimnion, which we substantiate with the following calculation: The stoichiometry of microbial methane oxidation is:



where  $y$  is the carbon use efficiency and  $CH_2O^{BM}$  designates MOB biomass. Based on theoretical considerations and experimental data, a carbon use efficiency of 0.4 has been reported (Leak and Dalton, 1986). This means that per mole of methane 1.6 moles of oxygen are used. The mixed layer depths for the four sampling campaigns are roughly 6, 10, 12 and 14 m, corresponding to mixed layer volumes of 2.5, 3.7, 4.1 and 4.3 GL in Lake Rotsee. Multiplying the measured methane oxidation rates in the epilimnion with these volumes results in a total methane oxidation of 600, 11560, 11800 and 200 mol d<sup>-1</sup>. Integrated over the time period of the four campaigns, this results in a total of 0.66 Mmol of methane that were oxidized with 1.1 Mmol of oxygen from the epilimnion. In an average volume of the mixed layer of 3.7 GL with an initial concentration of 340 μM (10.9 mg L<sup>-1</sup>) of oxygen, this would reduce the oxygen concentration by 180 μM to 160 μM or to about 5 mg L<sup>-1</sup>. Note that possible oxygen production and exchange with the atmosphere, as well as additional oxygen sinks are not included in these considerations.”

L 228 critical phase – critical for what?

Answer: We clarified that this phase is critical for potential outgassing to the atmosphere and thus for climate relevance. Section 3.4, L. 342.

L 233 specific affinity towards methane... unclear what is meant here.

Answer: We rephrased: “specific methane affinity”.

L 235 was the convergence only driven by changes in kinetic parameter in the epilimnion (or also in the hypolimnion as seems apparent from Fig. 2 a)

Answer: We clarified that the convergence was driven by changes in kinetic parameter in the epilimnion and the hypolimnion. L.351-356.

L 289 remove “as in many other stratified lakes” – too speculative (or include references, but I would not advise so in the conclusion part)

Answer: We provided references in the revised manuscript (L. 427).

That low methane concentrations are found in the epilimnion and higher methane concentrations in the hypolimnion is very common, especially in small lakes e.g. (Bastviken et al., 2004; Borrel et al., 2011), which can vary seasonally like in Rotsee, or in permanently stratified lakes elevated methane concentrations can persist over many decades. Continuing eutrophication of lakes and lack of recovery of eutrophic lakes will likely increase the number of lakes with anoxic methane-rich bottom waters in future (Beaulieu et al., 2019; Jenny et al., 2016).

We toned down the generalized claims at the end of the conclusion in the revised manuscript in order to put our results into context without overstating generalizability.

L 295 adaptation to oligotrophic conditions – Lake Rotsee can not be considered oligotrophic

Answer: What we mean is adaptation to low methane availability, we removed the term accordingly (L. 434).

L 298 transport of methane into the epilimnion provided and advantage for fast-growing

MOB over slower competitors. This is not shown (at least in this manuscript) and should be removed.

Answer: We have provided evidence for the dynamic adaptation in (Mayr et al., 2020), but the reviewer is correct that the phrasing here is misleading and while our data here is in line with the previous investigation the conclusion cannot be made from the data in this paper. We have rephrased this sentence in the revised manuscript and removed the respective part (L.436).

**References:**

- Bastviken, D., Cole, J. J., Pace, M. and Tranvik, L. J.: Methane emissions from lakes: Dependence of lake characteristics, two regional assessments, and a global estimate, *Global Biogeochem. Cycles*, 18(4), 1–12, doi:10.1029/2004GB002238, 2004.
- Beaulieu, J. J., DelSontro, T. and Downing, J. A.: Eutrophication will increase methane emissions from lakes and impoundments during the 21st century, *Nat. Commun.*, 10(1), 1375, doi:10.1038/s41467-019-09100-5, 2019.
- Borrel, G., Jézéquel, D., Biderre-Petit, C., Morel-Desrosiers, N., Morel, J. P., Peyret, P., Fonty, G. and Lehours, A. C.: Production and consumption of methane in freshwater lake ecosystems, *Res. Microbiol.*, 162(9), 833–847, doi:10.1016/j.resmic.2011.06.004, 2011.
- DelSontro, T., Beaulieu, J. J. and Downing, J. A.: Greenhouse gas emissions from lakes and impoundments: Upscaling in the face of global change, *Limnol. Oceanogr. Lett.*, 3(3), 64–75, doi:10.1002/lol2.10073, 2018.
- Jenny, J.-P., Francus, P., Normandeau, A., Lapointe, F., Perga, M. E., Ojala, A., Schimmelmann, A. and Zolitschka, B.: Global spread of hypoxia in freshwater ecosystems during the last three centuries is caused by rising local human pressure, *Glob. Chang. Biol.*, 22(4), 1481–1489, doi:10.1111/gcb.13193, 2016.
- Leak, D. J. and Dalton, H.: Growth yields of methanotrophs - 1. Effect of copper on the energetics of methane oxidation, *Appl. Microbiol. Biotechnol.*, 23(6), 470–476, doi:10.1007/BF02346062, 1986.
- Mayr, M. J., Zimmermann, M., Dey, J., Brand, A., Wehrli, B. and Bürgmann, H.: Growth and rapid succession of methanotrophs effectively limit methane release during lake overturn, *Commun. Biol.*, 3(1), 108, doi:10.1038/s42003-020-0838-z, 2020.

# Lake mixing regime selects apparent methane-oxidation kinetics of the methanotroph assemblage

Magdalena J. Mayr<sup>1,2\*</sup>, Matthias Zimmermann<sup>1,2\*</sup>, Jason Dey<sup>1</sup>, Bernhard Wehrli<sup>1,2</sup> and Helmut Bürgmann<sup>2</sup>

\* These authors contributed equally to this work.

<sup>1</sup>Department of Surface Waters—Research and Management, Eawag, Swiss Federal Institute of Aquatic Science and Technology, Kastanienbaum, Switzerland

<sup>2</sup>Institute of Biogeochemistry and Pollutant Dynamics, Department of Environmental Systems Science, ETH Zurich, Swiss Federal Institute of Technology, Zurich, Switzerland

Correspondence to: Magdalena J. Mayr (magdalena.mayr@eawag.ch)

**Abstract.** In ~~freshwater~~ lakes, large amounts of methane are produced in anoxic sediments. Methane-oxidizing bacteria effectively convert this potent greenhouse gas into biomass and carbon dioxide. These bacteria are present throughout the water column where methane concentrations can range from nanomolar to millimolar concentrations. In this study, we tested the hypothesis that methanotroph assemblages in a seasonally stratified ~~lakes~~freshwater lake are adapted to the contrasting methane concentrations in the epi- and hypolimnion. We further hypothesized that lake overturn would change the apparent methane oxidation kinetics as more methane becomes available in the epilimnion. Together with the change of methane oxidation kinetics, we investigated changes in the transcription of genes encoding methane monooxygenase, the enzyme responsible for the first step of methane oxidation, with metatranscriptomics. We show in laboratory incubations of the natural microbial communities that the half-saturation constant ( $K_m$ ) for methane, ~~obtained from laboratory experiments with the natural microbial community, differed by two orders of magnitude between epi- and~~ the methane concentration at which half the maximum methane oxidation rate is reached – was 20 times higher in the hypolimnion than in the epilimnion during stable stratification. During lake overturn, however, the kinetic constants in the epi- and hypolimnion converged along with a change of the transcriptionally active methanotroph assemblage. Conventional particulate methane monooxygenase appeared to be responsible for methane oxidation under different methane concentrations. Our results suggest that methane availability is one important factor for creating niches for methanotroph assemblages with well-adapted methane-oxidation kinetics. This rapid selection and succession of adapted lacustrine methanotroph assemblages ~~allows~~allowed the previously reported high ~~methane~~ removal efficiency of ~~more than~~ 90 % methane transported to the epilimnion to be maintained even under rapidly changing conditions during lake overturn. Consequently, only a small fraction of methane stored in the anoxic hypolimnion is emitted to the atmosphere.

Lakes are an important source of greenhouse gases with methane emissions contributing a major fraction to the climate impact of lacustrine systems (DelSontro et al., 2018). The oxidation of the strong greenhouse gas methane in freshwater lakes is mainly achieved by methane oxidizing bacteria (MOB), which have the unique ability to use methane as their sole carbon and energy source (Hanson and Hanson, 1996). In anoxic habitats of seasonally stratified lakes, large amounts of methane, which is produced as a final product of anaerobic organic matter degradation, can accumulate in the oxygen-depleted hypolimnion (Conrad, 2009; Steinsberger et al., 2017). Under stratified conditions, aerobic and sometimes anaerobic MOB oxidize this methane in the water column, thereby preventing diffusive outgassing (Bastviken et al., 2002; Graf et al., 2018; Mayr et al., 2019a). Lake overturn in autumn leads to mixing of the oxygen-rich surface layer with the methane-rich bottom water (Schubert et al., 2012). The simultaneous availability of oxygen and methane promotes growth of MOB in the expanding epilimnion at the surface (Kankaala et al., 2007; Mayr et al., 2019b; Schubert et al., 2012; Zimmermann et al., 2019). The resulting increase in methane oxidation capacity has been shown to be associated with a shift in the MOB assemblage in the epilimnion, which grows fast enough to prevent most of the methane transported into the epilimnion from escaping to the atmosphere (Mayr et al., 2019b; Zimmermann et al., 2019).

In temperate, seasonally stratified lakes, the diverse MOB assemblage shows a clear vertical structure and succession during autumn overturn (Kojima et al., 2009; Mayr et al., 2019b). This suggests that mechanisms of spatial and temporal niche partitioning maintain diversity within this functional group (Mayr et al., 2019a). The differences in the methane and oxygen availability in the two water bodies above and below the oxycline likely place very different demands on the ecophysiology of the resident MOB assemblages. Although previous studies have shown great diversity and adaptability of methane oxidation kinetics (Baani and Liesack, 2008; Dunfield and Conrad, 2000; Lofton et al., 2014; Tveit et al., 2019), the role of different kinetic traits in rapidly changing lake environments has so far not been studied systematically. Here, we hypothesized that kinetic parameters of methane oxidation vary between epi- and hypolimnion and that kinetic parameters vary seasonally together with the MOB assemblage, which would show that methane availability is a driver of methane oxidation kinetics of the MOB assemblage. Further, the methane affinity of lacustrine MOB especially in the epilimnion has implications for the amount of methane outgassing during both, stable stratification and lake overturn.

The first step of methane oxidation is mediated by the methane monooxygenase. Most MOB possess the copper-dependent particulate form of the methane monooxygenase (pMMO). Known isozymes of pMMO have been shown to exhibit different methane oxidation kinetics, including high affinity variants that are able to oxidize methane even at atmospheric concentrations (Baani and Liesack, 2008; Dam et al., 2012). A subset of MOB encode the soluble MMO (sMMO) that has a lower methane affinity than pMMO and has been hypothesized to be used by MOB under high methane concentration, because MOB biomass is assumed to be higher under such conditions leading to copper limitation and a switch to copper-free sMMO (Semrau et al., 2018). The abundance of the sMMO gene has been found to be low in a Lake Rotsee (Guggenheim et al., 2019), but relative transcription between epi- and hypolimnion has not been investigated so far.

Lakes are an important source of greenhouse gases. Methane is a major contributor to the climate impact of the greenhouse gas emissions from lakes (DelSontro et al., 2018). The oxidation of the strong greenhouse gas methane in freshwater lakes is mainly achieved by methane-oxidizing bacteria (MOB), which have the unique ability to use methane as their sole carbon and energy source (Hanson and Hanson, 1996). In seasonally stratified lakes, large amounts of methane, which is produced as a final product of anaerobic organic matter degradation, can accumulate in the oxygen-depleted hypolimnion (Conrad, 2009; Steinsberger et al., 2017). Under stratified conditions, aerobic and sometimes anaerobic MOB oxidize this methane in the water column, thereby preventing diffusive outgassing (Bastviken et al., 2002; Graf et al., 2018; Mayr et al., 2020a). Lake overturn in autumn leads to mixing of the oxygen-rich surface layer with the methane-rich bottom water (Schubert et al., 2012). The simultaneous availability of oxygen and methane promotes growth of MOB in the expanding epilimnion at the surface (Kankaala et al., 2007; Mayr et al., 2020b; Schubert et al., 2012; Zimmermann et al., 2019). The resulting increase in methane oxidation capacity has been shown to be associated with a shift in the MOB assemblage in the epilimnion, which grows fast enough to prevent 90% of the methane transported into the epilimnion from escaping to the atmosphere (Mayr et al., 2020b; Zimmermann et al., 2019).

81 In temperate, seasonally stratified lakes, the diverse MOB assemblage shows a clear vertical structure and  
82 succession during autumn overturn (Kojima et al., 2009; Mayr et al., 2020b). This suggests that mechanisms of  
83 spatial and temporal niche partitioning maintain diversity within this functional group (Mayr et al., 2020a). The  
84 differences in the methane and oxygen availability in the two water bodies above and below the oxycline likely  
85 place very different demands on the ecophysiology of the resident MOB assemblages. Although previous studies  
86 have shown great diversity and adaptability of methane oxidation kinetics (Baani and Liesack, 2008; Dunfield and  
87 Conrad, 2000; Lofton et al., 2014; Tveit et al., 2019), the role of different kinetic parameters in rapidly changing  
88 lake environments has so far not been studied systematically. Here, we hypothesized that apparent kinetic  
89 parameters of methane oxidation vary between epi- and hypolimnion and that kinetic parameters vary seasonally  
90 together with the MOB assemblage, which would show that methane availability is a driver of apparent methane  
91 oxidation kinetics of the MOB assemblage. Further, the methane affinity of lacustrine MOB especially in the  
92 epilimnion has implications for the amount of methane outgassing during both, stable stratification and lake  
93 overturn.

94 The first step of methane oxidation is mediated by the methane monooxygenase. Most MOB possess the copper-  
95 dependent particulate form of the methane monooxygenase (pMMO). Known isozymes of pMMO have been  
96 shown to exhibit different methane oxidation kinetics, including high affinity variants that are able to oxidize  
97 methane even at atmospheric concentrations (Baani and Liesack, 2008; Dam et al., 2012). A subset of MOB encode  
98 the soluble MMO (sMMO) that has a lower methane affinity than pMMO and has been hypothesized to be used by  
99 MOB under high methane concentration, because MOB biomass is assumed to be higher under such conditions  
100 leading to copper limitation and a switch to copper-free sMMO (Semrau et al., 2018). The abundance of the sMMO  
101 gene has been found to be low in Lake Rotsee (Guggenheim et al., 2019), but relative transcription between epi-  
102 and hypolimnion has not been investigated so far.

103 In this study we conducted a combined kinetic and metatranscriptomic analysis in a small pre-alpine lake to test  
104 our hypothesis that MOB assemblages show distinct apparent methane oxidation kinetics in the methane-rich  
105 hypolimnion compared to the epilimnion with low methane concentrations. Further, we examined the changes in  
106 apparent methane oxidation kinetics over time during lake overturn, as more methane becomes available in the  
107 epilimnion. To do so, we used ex-situ laboratory incubations of the resident microbial community to measure  
108 methane-oxidation rates and methane affinity combined with MOB cell counts. In parallel, we applied  
109 metagenomics and metatranscriptomics to characterize the MOB assemblage and as well as genes and transcripts  
110 involved in the methane oxidation pathway, aiming to link observed changes in apparent methane oxidation kinetics  
111 with changes in the MOB population activity. Knowledge about the variability of kinetic parameters of methane  
112 oxidation is important to better understand the ecology and physiology of MOB in the environment. Further, our  
113 results will inform trait-based or process-based modelling approaches, because a single set of time and space  
114 invariant kinetic parameters may not reflect natural conditions adequately.

## 115 2 Methods

### 116 2.1 Study site and physicochemical lake profiling

117 Lake Rotsee is a small eutrophic lake in central Switzerland that is 2.5 km long, 200 m wide and has a maximum  
118 depth of 16 m. ~~For more details see (Schubert et al., 2012). We profiled and sampled the water column during five~~  
119 ~~campaigns in autumn 2017 at the deepest point of Lake Rotsee at 47.072 N and 8.319 E. We measured profiles of~~  
120 ~~temperature, conductivity~~ For more details see Schubert et al. (2012). We profiled and sampled the water column  
121 during four campaigns in autumn 2017 at the deepest point of Lake Rotsee at 47.072 N and 8.319 E. We measured  
122 profiles of temperature and pressure (depth) with a CTD (RBRmaestro, RBR, Canada). A micro-optode (NTH-  
123 PSt1, PreSens, Germany) attached to the CTD measured profiles of oxygen concentrations.

### 124 2.2 <sup>3</sup>H-CH<sub>4</sub> tracer technique

125 ~~We used the radio-<sup>3</sup>H-CH<sub>4</sub> tracer technique as described in Bussmann et al., (2015) and Steinle et al., (2015) to~~  
126 ~~measure methane oxidation rates and kinetics of the MOB assemblage above and below the oxycline. We added~~  
127 ~~200 μL of gaseous <sup>3</sup>H-CH<sub>4</sub>/N<sub>2</sub> mixture (~80 kBq, American Radiolabeled Chemicals, USA). We measured total~~

and water fraction radioactivity in a liquid scintillation counter (Tri-Carb 1600CA, Packard, USA) by adding 1 mL sample to 5 mL Insta-Gel (PerkinElmer, Germany). From these activities, we calculated the methane oxidation rate ( $r_{MOx}$ ):

$$r_{MOx} = [CH_4] \times \frac{A_{H_2O}}{A_{H_2O} + A_{CH_4}} \times \frac{1}{t}$$

where  $t$  is time,  $[CH_4]$  is the concentration of methane and activities ( $A$ ) were corrected for fractional turnover in killed controls.

**2.3 Methane oxidation kinetics** We used the radio  $^3H$ - $CH_4$  tracer technique as described in Bussmann et al. (2015) and Steinle et al. (2015) to measure apparent methane oxidation rates and kinetics of the MOB assemblage above and below the oxycline. Similar measurements have been done by Lofton et al. (2014), who derived apparent methane oxidation kinetics from methane oxidation rates using  $^{14}C$ - $CH_4$ . We used the  $^3H$ - $CH_4$  tracer technique because it is more sensitive than the  $^{14}C$ - $CH_4$  technique and therefore allows shorter incubation times and rate determination at low  $CH_4$  concentrations. We added 200  $\mu$ L of gaseous  $^3H$ - $CH_4/N_2$  mixture (~80 kBq, American Radiolabeled Chemicals, USA). The specific activity of  $^3H$ - $CH_4$  is 0.74 TBq  $mmol^{-1}$  and the 200  $\mu$ L of gaseous  $^3H$ - $CH_4/N_2$  mixture therefore contained 108 pmol  $^3H$ - $CH_4$ . In comparison, the 500  $\mu$ L gas bubble with the lowest concentration of unlabelled methane (see section 2.3), contained 17 nmol  $CH_4$ . We measured total and water fraction radioactivity in a liquid scintillation counter (Tri-Carb 1600CA, Packard, USA) by adding 1 mL sample to 5 mL Insta-Gel (PerkinElmer, Germany). From these activities, we calculated the methane oxidation rate ( $r_{MOx}$ ):

$$r_{MOx} = [CH_4] \times \frac{A_{H_2O}}{A_{H_2O} + A_{CH_4}} \times \frac{1}{t}$$

where  $t$  is time,  $[CH_4]$  is the concentration of methane and activities ( $A$ ) were corrected for fractional turnover in killed controls.

### **2.3 Apparent methane oxidation kinetics of microbial community communities**

We assumed that the dependence of the methane oxidation rate ( $r_{MOx}$ ) of the microbial community on the methane concentration can be described by a Monod kinetics:

$$r_{MOx} = V_{max} \frac{[CH_4]}{K_M + [CH_4]}$$

where  $V_{max}$  is the maximum methane oxidation rate and  $K_M$  is the half-saturation constant for methane. We use the term *affinity* as the inverse of the half-saturation constant:  $1/K_m$ . We determined the two kinetic parameters in *ex-situ* laboratory incubations of water samples from above and below the oxycline. We collected water from the two depths in 2 L Schott bottles and transported them to the lab dark and cooled. We stripped dissolved methane by bubbling air for 1h. This also removed  $H_2S$  from the sample which would otherwise reduce the sensitivity of the  $^3H$ - $CH_4$  technique. For each depth, we prepared 60 mL incubations with 10 different methane concentrations and a killed control in duplicates. We prepared incubations and controls in triplicates except for the first field campaign where we only prepared duplicates. By adding a 500  $\mu$ L gas bubble from pre-diluted gas stocks we established methane concentrations of 0.4 to 60  $\mu$ M. Gas stocks were prepared by evacuating and flushing 120 mL crimp-sealed serum vials with pure nitrogen gas five times and adding defined volumes of methane gas with gas tight syringes. In the killed controls, we treated in the exact same way as the samples with the exception that we inhibited methane oxidation by adding 1 mL of  $ZnCl_2$  (50 % w/v). To start the incubations, we added the  $^3H$ - $CH_4$  tracer as described in the above section. After vigorous shaking for 1 minute, we kept the incubations dark in a shaker with 100 RPM. We incubated both samples from above and below the oxycline at the same temperature as measured within the oxycline. While the determined kinetic parameters may thus differ from in-situ values, this approach allows for a direct comparison of the two datasets. After 4 hours, we stopped the incubations by adding 1 mL of  $ZnCl_2$  (50 % w/v). We determined the methane oxidation rate in each incubation as described above. Except for the first sampling date, we measured each incubation replicate twice. This resulted in 594 measurements, 72 single measurements and 261 measurement duplicates. We averaged measurement replicates resulting in 333 data points.

We used a non-linear least squares Levenberg-Marquardt algorithm to fit the Monod equation to the data. Outliers in the data were removed using the following criteria: For the replicates of each methane concentration we removed data points (1) with a water fraction radioactivity that was outside  $2\sigma$  from the average water fraction radioactivity of all replicates, (2) which showed a water fraction radioactivity that was not above  $2\sigma$  from the background water fraction radioactivity, (3) for which we had less than two replicates after the removal of outliers, (4) with a resulting methane oxidation rate outside  $2\sigma$  from the average methane oxidation rate of all replicates, and (5) showing a methane oxidation rate that was higher than the methane oxidation rate measured for the replicates with the highest methane concentration. [The  \$2\sigma\$  approach is one recommended approach for outlier detection \(e.g. Leys et al., 2013\). Because we only had incubation duplicates for the first sampling date, it was not possible to detect outliers based on  \$2\sigma\$  for this campaign and we kept both values in the analysis. The average water fraction radioactivity of the killed controls was used as background radioactivity in the outlier detection procedure. In total 221 datapoints were finally considered in the analysis \(66% of all datapoints without measurement replicates\). For the five individual outlier criteria, the percentages of detected outliers are: \(1\) 4%, \(2\) 4%, \(3\) 3%, \(4\) 19%, \(5\) 3%. The high percentage of outliers for criteria 4 is related to the fact that methane oxidation rates are associated with a higher error than individual measurements because they are computed from multiple individual measurements.](#)

The base value of the *specific affinity*  $a^\circ$  is defined as the ratio  $V_{max}/K_M$ . We approximated mean and variance of the ratio of the two random variables with known mean and variance using the Taylor expansions given in [ref. \(Stuart and Ord, 2009\).Stuart and Ord \(2009\).](#)

## 2.4 ~~In-situ methane~~Methane oxidation rates of the microbial community

We determined the ~~in-situ~~ methane oxidation rate of the natural microbial community in duplicate ~~ex-situ~~laboratory incubations of water samples from above and below the oxycline. We anaerobically filled water into 60 mL serum vials, and crimp-sealed and transported them to the lab dark and cooled. For each depth, we prepared killed controls with 1 mL of  $ZnCl_2$  (50 % w/v) in duplicates in the same way. We started the incubations by adding the  $^3H-CH_4$  tracer as described above. After vigorous shaking for 1 minute, we kept the incubations dark in a shaker with 100 RPM at the temperature measured within the oxycline. After 4 hours, we stopped the incubations by adding 1 mL of  $ZnCl_2$  (50 % w/v).

## 2.5 Methane concentration measurement

We measured *in-situ* methane concentrations in the water column using the headspace equilibration method. For each depth, we collected water samples in 120 mL crimp-sealed serum vials with a small amount of  $CuCl_2$  to ~~stop~~ biological activity. ~~We measured methane concentrations in the headspace with a gas chromatograph (Agilent 6890N, USA) equipped with a Carboxen 1010 column (Supelco 10 m  $\times$  0.53 mm, USA) and flame ionisation detector. Samples that exceeded the calibration range were diluted with  $N_2$  and measured again. We calculated dissolved methane concentrations according to Wiesenburg and Guinasso, (1979).~~stop biological activity. We measured methane concentrations in the headspace with a gas chromatograph (Agilent 6890N, USA) equipped with a Carboxen 1010 column (Supelco 10 m  $\times$  0.53 mm, USA) and flame ionisation detector. Samples that exceeded the calibration range were diluted with  $N_2$  and measured again. We calculated dissolved methane concentrations according to Wiesenburg and Guinasso (1979).

## 2.6 Quantification of methanotroph cells

~~We investigated the abundance of aerobic methanotrophs by catalysed reporter deposition fluorescence in situ hybridisation after Pernthaler et al., (2002). We fixed water samples of 5 mL with 300  $\mu$ L sterile filtered (0.2  $\mu$ m) formaldehyde (2.22% v/v final concentration) for 3–6 h on ice. We filtered the samples onto 0.2  $\mu$ m nucleopore track-etched polycarbonate membrane filters (Whatman, UK), that we dried, and stored at  $-20^\circ C$  until further analysis. We permeabilized cells with lysozyme (10 mg  $mL^{-1}$ ) at  $37^\circ C$  for 70 min, and inactivated endogenous peroxidases with 10 mM HCl for 10 min at room temperature. To hybridise the filters, we used a hybridisation buffer (Eller et al., 2001) containing HRP-labelled probes at  $46^\circ C$  for 2.5 h. Furthermore, the buffer contained either a 1:1:1 mix of Mg84, Mg705, and Mg669 probes targeting methanotrophic *Gammaproteobacteria* or a Ma450 probe targeting methanotrophic *Alphaproteobacteria* (Eller et al., 2001). To amplify the fluorescent signals, we used the green fluorescent Oregon Green 488 tyramide (OG) fluorochrome (1  $\mu$ L  $mL^{-1}$ ) at  $37^\circ C$  for~~

220 30 min. We counterstained hybridised cells with DAPI (20  $\mu\text{l}$  of 1  $\mu\text{g mL}^{-1}$  per filter) for 5 minutes. For  
221 microscopy, we used a 4:1 mix of Citifluor AF1 (Electron Microscopy Sciences, Hatfield, PA, USA) and  
222 Vectashield (Vector, Burlingame, CA, USA) as mountant. We used an inverted light microscope (Leica  
223 DMI6000 B, Germany) at a 1000 fold magnification to quantify MOB cell numbers. For each sample, we took 22  
224 image pairs (DAPI and OG filters) of randomly selected fields of view (FOVs). To detect and count cells we used  
225 digital microbial image analysis software Daime 2.0 (Daims, 2009).

226 We investigated the abundance of aerobic methanotrophs by catalysed reporter deposition fluorescence in situ  
227 hybridisation after Pernthaler et al. (2002). We fixed water samples of 5 mL with 300  $\mu\text{l}$  sterile filtered (0.2  $\mu\text{m}$ )  
228 formaldehyde (2.22% v/v final concentration) for 3 – 6 h on ice. We filtered the samples onto 0.2  $\mu\text{m}$  nucleopore  
229 track-etched polycarbonate membrane filters (Whatman, UK), that we dried, and stored at -20 °C until further  
230 analysis. We permeabilized cells with lysozyme (10  $\text{mg mL}^{-1}$ ) at 37 °C for 70 min, and inactivated endogenous  
231 peroxidases with 10 mM HCl for 10 min at room temperature. To hybridise the filters, we used a hybridisation  
232 buffer (Eller et al., 2001) containing HRP-labelled probes at 46 °C for 2.5 h. Furthermore, the buffer contained  
233 either a 1:1:1 mix of Mg84, Mg705, and Mg669 probes targeting methanotrophic *Gammaproteobacteria* or a  
234 Ma450 probe targeting methanotrophic *Alphaproteobacteria* (Eller et al., 2001). To amplify the fluorescent signals,  
235 we used the green-fluorescent Oregon Green 488 tyramide (OG) fluorochrome (1  $\mu\text{l mL}^{-1}$ ) at 37 °C for 30 min. We  
236 counterstained hybridised cells with DAPI (20  $\mu\text{l}$  of 1  $\mu\text{g mL}^{-1}$  per filter) for 5 minutes. For microscopy, we used  
237 a 4:1 mix of Citifluor AF1 (Electron Microscopy Sciences, Hatfield, PA, USA) and Vectashield (Vector,  
238 Burlingame, CA, USA) as mountant. We used an inverted light microscope (Leica DMI6000 B, Germany) at a  
239 1000-fold magnification to quantify MOB cell numbers. For each sample, we took 22 image pairs (DAPI and OG  
240 filters) of randomly selected fields of view (FOVs). To detect and count cells we used digital microbial image  
241 analysis software Daime 2.0 (Daims, 2009).

## 242 2.7 Metagenome and metatranscriptome analysis

243 We collected lake water with a Niskin bottle and filtered 800 – 2300ml on-site onto 0.2  $\mu\text{m}$  pore size GTTP isopore  
244 filters (Merck Millipore Ltd.). ~~These~~To keep the filtration time as short as possible (typically <10 min) and at the  
245 same time retrieve enough RNA for sequencing, a 142 mm diameter filter was used. To minimize sample  
246 perturbation the filtration device was connected directly to the Niskin bottle. The filters were preserved immediately  
247 on dry ice and stored at -80 °C until extraction. ~~We did not apply prefiltration, because filamentous methanotrophs~~  
248 ~~can reach lengths of >100  $\mu\text{m}$  (Oswald et al., 2017).~~ We extracted DNA and RNA with the Allprep DNA/RNA  
249 Mini Kit (Qiagen) and treated RNA with the rigorous option using the Turbo DNA-free kit (Invitrogen) to remove  
250 remaining DNA. ~~In~~To increase the confidence in the measurement a second filter of the January ~~two filters of the~~  
251 hypolimnion sample ~~were~~was extracted and sequenced separately ~~–~~ ~~servicing~~. ~~This replicate is shown as replicates~~  
252 ~~indicated with~~ Jan (r). RNA yields from the October sampling were deemed insufficient for sequencing as no  
253 typical RNA bands were visible during quality control and therefore these samples were omitted from  
254 metatranscriptome analysis. Metagenomic and metatranscriptomic 150bp paired-end sequencing was done on a  
255 NovaSeq 6000 sequencer (Illumina) at Novogene (HK) company limited (Hong Kong, China). Ribosomal RNA  
256 was depleted with Ribo-Zero Magnetic Kit (Illumina) prior to sequencing. The co-assembly of metagenomic  
257 sequences alone yielded less *pmoA* as well as *pmoB* and *pmoC* sequences than expected, likely due to low coverage.  
258 Therefore, we combined predicted genes from both the metagenomic and the metatranscriptomic *de-novo* assembly  
259 as described below. Due to low coverage of *pmoA*, *pmoB* and *pmoC* in the metagenome, we used the metagenome  
260 only in the assembly process. All further analyses relied on the metatranscriptome.

261 ~~We removed remaining ribosomal sequences from metatranscriptomic reads with sortmerna v2.1 (Kopylova et~~  
262 ~~al., 2012) and performed quality filtering with trimmomatic v0.35 (Bolger et al., 2014). We co-assembled reads~~  
263 ~~from seven metatranscriptomic libraries using megahit v1.1.3 (Li et al., 2015) with a final k-mer size of 141 and a~~  
264 ~~minimum contig length of 200. This resulted in 2166829 contigs with an average of 672bp and a N50 of 733bp.~~  
265 ~~For quality filtering of metagenomic reads we used prinseq-lite v0.20.4 (Schmieder and Edwards, 2011) with dust~~  
266 ~~filter (30) and a quality mean of 20. Again we performed a co-assembly using megahit of 10 metagenomes~~  
267 ~~(including three October samples without corresponding metatranscriptome) with a final k-mer size of 121 and a~~  
268 ~~minimum contig size of 300bp (4237394 contigs, average 1008bp and N50 of 1250bp). Gene prediction for both~~  
269 ~~co-assemblies was done with prodigal v 2.6.3 (setting: meta, Hyatt et al., 2010). After combining the predicted~~  
270 ~~genes, cd-hit-est v4.6.6 (Li and Godzik, 2006) was used to remove very similar and duplicate (identity 0.99)~~

271 predicted genes. With Seqkit v0.7.2 (Shen et al., 2016) predicted genes shorter than 400bp were removed.  
272 Predicted genes encoding particulate methane monooxygenases were annotated with prokka v1.3 (Seemann,  
273 2014) using the incorporated databases (metagenome option) and diamond blastx v0.9.22 (e-value  $10^{-6}$ , Buchfink  
274 et al., 2014) against custom databases for *pmoA*, *pmoB* and *pmoC*. Annotation was manually validated using  
275 alignments and the NCBI refseq protein database (22.4.2019, O'Leary et al., 2016). *pmoA*, *pmoB* and *pmoC*  
276 variants summing to a cross-sample sum higher than 50 transcripts per million (TPM) were retained. Genes  
277 annotated as *pmoA*, *pmoB* and *pmoC* variants which were either not the expected gene (manual inspection) or  
278 shorter than 300 bp were removed. Genes encoding part of the soluble methane monooxygenase sMMO (*mmoX*,  
279 *mmoY* and *mmoZ*) were annotated with prokka v1.3 using incorporated databases and the metagenome option.  
280 Paired-end metatranscriptomic reads were mapped to the predicted genes using bbmap v35.85 (Bushnell, 2014) at  
281 an identity of 0.99 without mapping of ambiguous reads, and then converted with samtools v1.9 (Li et al., 2009)  
282 and counted with featurecounts (Liao et al., 2014) of subread v1.6.4 package (-p option). The count table was  
283 normalized within samples to transcripts per million (TPM, Wagner et al., 2012) by first dividing the counts by  
284 gene length, then the result by gene was divided by the sum of all results times one million. The TPM values  
285 were used to produce the figures in R.

286 We removed remaining ribosomal sequences from metatranscriptomic reads with sortmerna v2.1 (Kopylova et al.,  
287 2012) and performed quality filtering with trimmomatic v0.35 (Bolger et al., 2014), resulting in 26.6 million - 34  
288 million high quality reads. We co-assembled reads from seven metatranscriptomic libraries using megahit v1.1.3  
289 (Li et al., 2015) with a final k-mer size of 141 and a minimum contig length of 200. This resulted in 2166829  
290 contigs with an average of 672bp and a N50 of 733bp. For quality filtering of metagenomic reads we used prinseq-  
291 lite v0.20.4 (Schmieder and Edwards, 2011) with dust filter (30) and a quality mean of 20, resulting in 31.1 million  
292 - 37.1 million high quality reads. Again, we performed a co-assembly using megahit of 10 metagenomes (including  
293 three October samples without corresponding metatranscriptome) with a final k-mer size of 121 and a minimum  
294 contig size of 300bp (4237394 contigs, average 1008bp and N50 of 1250bp). We measured one additional depth in  
295 October in between epi- and hypolimnion, which is included in the data repository but is not discussed here. We  
296 did not pursue the intermediate sample in later campaigns since we focused our effort on the epilimnion and  
297 hypolimnion (continuing with measurement triplicates). We did however use the metagenomics data from this  
298 sample for the assembly. Gene prediction for both co-assemblies was done with prodigal v 2.6.3 (setting: meta,  
299 Hyatt et al., 2010). After combining the predicted genes, cd-hit-est v4.6.6 (Li and Godzik, 2006) was used to  
300 remove very similar and duplicate (identity 0.99) predicted genes. With Seqkit v0.7.2 (Shen et al., 2016) predicted  
301 genes shorter than 400bp were removed. Predicted genes encoding pMMO were annotated with prokka v1.3  
302 (Seemann, 2014) using the incorporated databases (metagenome option) and diamond blastx v0.9.22 (e-value  $10^{-6}$ ,  
303 Buchfink et al., 2014) against custom databases for *pmoA*, *pmoB* and *pmoC*. These custom databases included  
304 *pxmABC*, *pmoCAB2*, *pmoCAB* from both alpha- and gammaproteobacterial genomes, which were extracted  
305 manually. The databases are provided as supplementary files 1-3. Annotation was manually validated using  
306 alignments and the NCBI refseq protein database (22.4.2019, O'Leary et al., 2016). *pmoA*, *pmoB* and *pmoC*  
307 variants summing to a cross-sample sum higher than 50 transcripts per million (TPM) were retained. Genes  
308 annotated as *pmoA*, *pmoB* and *pmoC* variants which were either not the expected gene (manual inspection) or  
309 shorter than 400 bp were removed. Genes encoding part of the soluble methane monooxygenase sMMO (*mmoX*,  
310 *mmoY* and *mmoZ*) were annotated with prokka v1.3 using incorporated databases and the metagenome option.  
311 Paired-end metatranscriptomic reads were mapped to the predicted genes using bbmap v35.85 (Bushnell, 2014) at  
312 an identity of 0.99 without mapping of ambiguous reads, and then converted with samtools v1.9 (Li et al., 2009)  
313 and counted with featurecounts (Liao et al., 2014) of subread v1.6.4 package (-p option). The count table was  
314 normalized within samples to transcripts per million (TPM, Wagner et al., 2012) by first dividing the counts by  
315 gene length, then the result by gene was divided by the sum of all results times one million. The TPM values (suppl.  
316 file 4) were used to produce the figures in R. The correspondence analysis (CA) was performed with vegan (v2.5.6,  
317 Oksanen et al., 2019) in R (v3.5.2, R Core Team, 2018) based on the combined and square root transformed TPM  
318 values of *pmoCAB* data (scaling=2).

319 All sequences were classified to the family level based on the NCBI refseq protein database using blastx (O'Leary  
320 et al., 2016). Further classification was based on a *pmoA* phylogenetic tree (shown in the supplementary material).  
321 *pmoA* amino acid sequences were derived with MEGA7 and aligned with Muscle (Kumar et al., 2016). A neighbor-  
322 joining tree was inferred using 10000 bootstrap replications with Poisson correction method based on 131 positions.

Known cultivated or uncultivated groups were assigned at bootstrap values >0.7 and a protein similarity >94%, corresponding to genus level resolution according to Knief (2015). The *pmoB* and *pmoC* sequences were assigned to these groups if originating from the same contig. For many sequences a more detailed taxonomic assignment than family was not possible, and therefore labelled “unclassified type Ia” and “unclassified type II”, respectively.

### 3 Results and discussion

#### 3.1 Environmental conditions during the autumn overturn

From October 2017 to January 2018 the epilimnion depth in Lake Rotsee gradually increased from 5.5 to 13.7 m (Fig. 1a-d). This process of vertical mixing continuously transferred methane that was stored below the oxycline into the epilimnion above. The gradual progression of the autumn overturn stimulates the growth of a distinct MOB assemblage in the epilimnion above the oxycline in response to an influx of methane from the hypolimnion as shown in previous work of Lake Rotsee (Mayr et al., 2019b; Zimmermann et al., 2019). Despite this continuous supply, measured methane concentrations above the oxycline remained below 1 µM (Fig. 1a-d, orange arrows). The low methane concentrations are an indication of intense methane oxidation by the growing MOB assemblage in the epilimnion. The oxygen concentration shifted from 15% oversaturation in October to 67% undersaturation in December (Fig. 1a-d). Aerobic methane oxidation likely contributed to this oxygen depletion in the epilimnion. In the hypolimnion oxygen concentrations were found to be below the detection limit (20 nM) (Kirf et al., 2014) from October to December. However, oxygen may be produced in the hypolimnion by phytoplankton (Brand et al., 2016; Oswald et al., 2015).

Lakes located in climatic zones with strong seasonal variability, show seasonal vertical stratification of their water masses that is fundamental for all physical, chemical and biological processes occurring within them (Boehrer and Schultze, 2008). During the warm season, the increasing temperature at the lake surface establishes two physically and chemically different water masses in the lake, the epilimnion and the hypolimnion. The epilimnion at the surface is warmer, well-mixed and has continuous supply of oxygen from the atmosphere and photosynthesis. In contrast, the colder and denser hypolimnion is physically separated from the epilimnion and generally shows diffusive gradients of dissolved substances. During the cold season, surface cooling leads to vertical mixing which gradually deepens the well-mixed surface layer and mixes hypolimnetic water into the surface layer. During this autumnal overturn period, both temperature and chemistry of the surface water change and potentially create new ecological niches. In the following we label the water masses above and below the thermocline as ‘epilimnion’ and ‘hypolimnion’. Even though the hypolimnion exhibits considerable internal chemical gradients, previous work has shown that the MOB assemblage is fairly homogeneous throughout the hypolimnion (Mayr et al., 2020b). In January, the lake was completely mixed. To be consistent with the previous sampling campaigns we still took two samples from different depths and refer to them as epilimnion and hypolimnion for convenience.

From October 2017 to January 2018 the epilimnion depth in Lake Rotsee gradually increased from 5.5 to 13.7 m (Fig. 1a-d). This process of vertical mixing continuously transferred methane that was stored below the thermocline into the epilimnion above. The gradual progression of the autumn overturn stimulates the growth of a distinct MOB assemblage in the epilimnion above the thermocline in response to an influx of methane from the hypolimnion as shown in previous work of Lake Rotsee (Mayr et al., 2020b; Zimmermann et al., 2019). Despite this continuous supply, measured methane concentrations above the thermocline remained below 1 µM (Fig. 1a-d, orange arrows). The low methane concentrations are an indication of intense methane oxidation by the growing MOB assemblage in the epilimnion. The oxygen concentration shifted from 15% oversaturation in October to 67% undersaturation in December (Fig. 1a-d). Aerobic methane oxidation likely contributed to the oxygen depletion in the epilimnion, which we substantiate with the following calculation: The stoichiometry of microbial methane oxidation is:



where  $y$  is the carbon use efficiency and  $CH_2O^{BM}$  designates MOB biomass. Based on theoretical considerations and experimental data, a carbon use efficiency of 0.4 has been reported (Leak and Dalton, 1986). This means that per mole of methane 1.6 moles of oxygen are used. The mixed layer depths for the four sampling campaigns are roughly 6, 10, 12 and 14 m, corresponding to mixed layer volumes of 2.5, 3.7, 4.1 and 4.3 GL in Lake Rotsee. Multiplying the measured methane oxidation rates in the epilimnion with these volumes results in a total methane

371 [oxidation of 600, 11560, 11800 and 200 mol d<sup>-1</sup>. Integrated over the time period of the four campaigns, this results](#)  
372 [in a total of 0.66 Mmol of methane that were oxidized with 1.1 Mmol of oxygen from the epilimnion. In an average](#)  
373 [volume of the mixed layer of 3.7 GL with an initial concentration of 340 μM \(10.9 mg L<sup>-1</sup>\) of oxygen, this would](#)  
374 [reduce the oxygen concentration by 180 μM to 160 μM or to about 5 mg L<sup>-1</sup>. Note that possible oxygen production](#)  
375 [and exchange with the atmosphere, as well as additional oxygen sinks are not included in these considerations. In](#)  
376 [the hypolimnion oxygen concentrations were below the detection limit \(20 nM\) \(Kirf et al., 2014\) from October to](#)  
377 [December. However, oxygen may be produced in the hypolimnion by phytoplankton \(Brand et al., 2016; Oswald](#)  
378 [et al., 2015\).](#)

379 The two water bodies above and below the ~~oxycline~~[thermocline](#) have distinct biogeochemical conditions posing  
380 very different demands on the ecophysiology of the MOB assemblage. The hypolimnion contained up to ~~a~~  
381 ~~few~~[several](#) hundred micromolar of methane but the flux of oxygen into the hypolimnion was limited due to  
382 stratification and low light levels for photosynthesis. On the other hand, the epilimnion contained comparably high  
383 oxygen concentrations, but methane concentrations remained low as methane was supplied slowly and was rapidly  
384 diluted in the large volume of the epilimnion. In addition, the temperature of the epilimnion dropped from 16 °C  
385 to 5 °C, whereas the hypolimnion remained cold (5 - 8 °C). ~~Temperature profiles are shown in Supplementary Fig.~~  
386 ~~4~~—A previous study investigating 16S rRNA genes and *pmoA* transcripts indeed revealed niche differentiation of  
387 the MOB assemblage ~~between the two water bodies above and below the oxycline with a shift in the MOB~~  
388 ~~assemblage during the overturn (Mayr et al., 2019b)~~ above and below the oxycline of Lake Rotsee with a shift in  
389 ~~the MOB assemblage during the overturn (Mayr et al., 2020b).~~

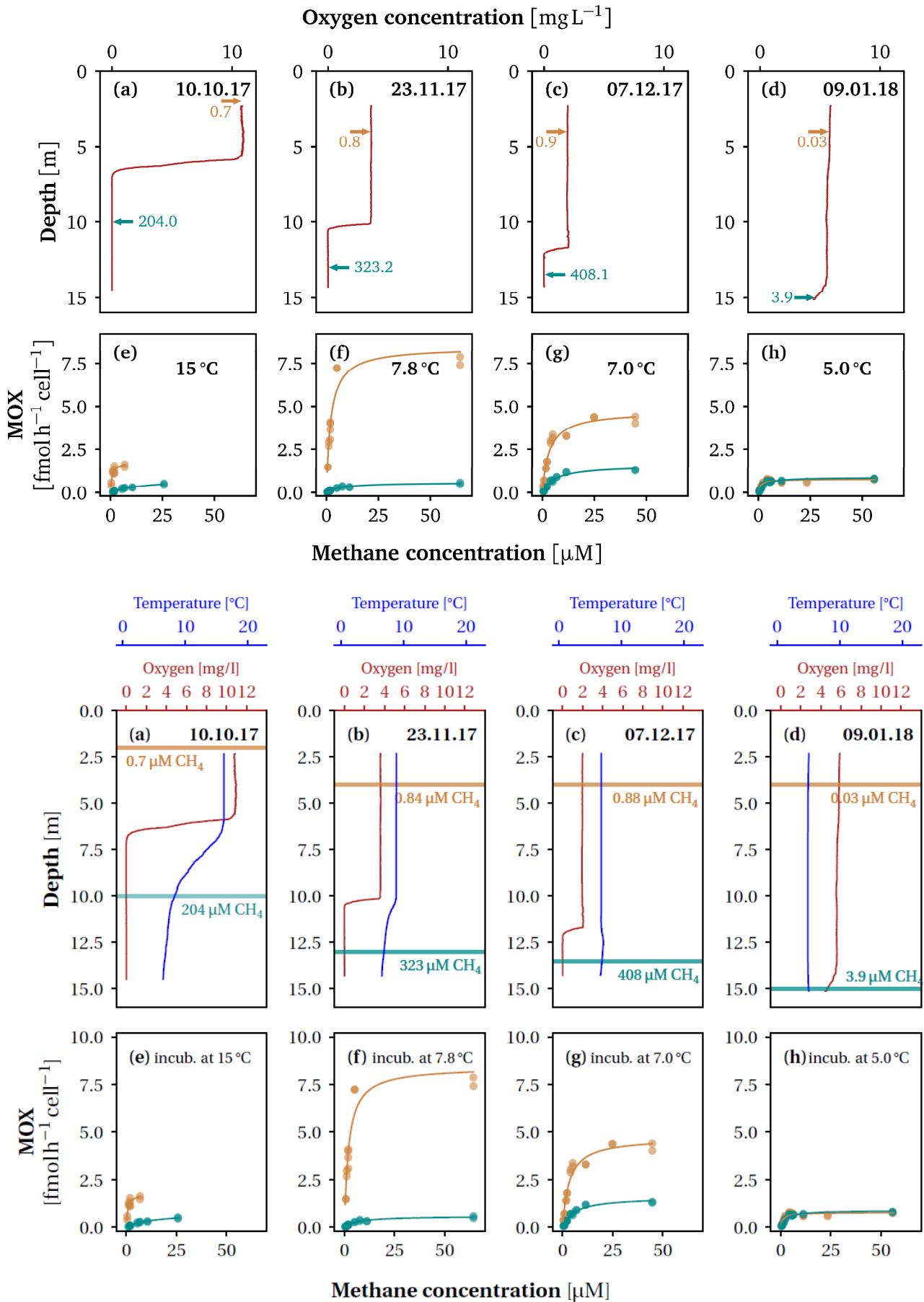


Figure 1. Substrate concentrations and [apparent methane oxidation rates kinetics](#) during lake overturn in [Lake Rotsee](#). (a - d) Oxygen concentration [and temperature](#) profiles during the four field campaigns at the dates indicated. The sampling depths

above (orange) and below (cyan) the oxycline are indicated by ~~arrows~~a horizontal bar. Numbers next to the ~~arrows~~bars represent methane concentrations in  $\mu\text{M}$  at the respective depths. (e - h) Cell-specific methane oxidation rates (MOX) of water samples incubated with different methane concentrations. Lines indicate least-square fits of the Monod kinetics. For each campaign, we incubated samples from both depths close to ~~in-situ~~temperature (~~indicated in bold~~), given next to the annotation (incub. = incubated).

### 390 3.2 Succession of kinetically different microbial communities

391 Along with the differences in the physical and chemical properties of the two water bodies, we observed a  
392 significant difference in the apparent methane oxidation kinetics of the MOB assemblages. From the methane  
393 oxidation rates shown in Fig. 1e-h we derived the parameters of Monod kinetics (Fig. 2). ~~These kinetic parameters~~  
394 In an attempt to measure methane kinetics under as standardized conditions as possible we measured samples from  
395 both depths under equal temperature and oxygen conditions. This allowed us to ~~characterize~~compare the  
396 physiological traits of the MOB assemblages above and below the oxycline ~~physiologically~~ and to relate these  
397 results to the biogeochemical conditions. ~~However, the parameters therefore do not necessarily represent the~~  
398 effective in-situ kinetics.

399 The curves describing the apparent methane oxidation kinetics of the MOB assemblages above and below the  
400 oxycline did not intersect (except at the origin) in October and November (Fig. 1e-g). This means that the MOB  
401 assemblage in the epilimnion showed both a higher *affinity* for methane (Fig. 2a) and a higher cell-specific  
402 maximum methane oxidation rate (Fig. 2b) than the assemblage below the oxycline. ~~The higher methane affinity~~  
403 ~~is in line with the methane-deficient conditions in the epilimnion. But the~~The fact that both *affinity* and maximum  
404 rate are higher ~~would by itself~~ suggests that the assemblage in the epilimnion has a competitive advantage over the  
405 assemblage in the hypolimnion. This implies that there were likely additional mechanisms or traits, like adaptation  
406 to oxygen concentration or temperature (~~Hernandez et al., 2015; Trotsenko and Khmelenina, 2005~~), ~~that~~  
407 ~~prevent~~(Hernandez et al., 2015; Trotsenko and Khmelenina, 2005), that prevented the epilimnetic MOB assemblage  
408 from invading the assemblage in the hypolimnion. ~~At the end of the overturn period (Fig. 1h) both MOB~~  
409 ~~assemblages showed very similar methane oxidation kinetics. We already have strong indications from our previous~~  
410 work that these factors are indeed important (Mayr et al., 2020b, 2020a).

411 ~~The pronounced difference in  $K_m$  of the two assemblages in October, when the lake was still stratified, gradually~~  
412 ~~converged during lake overturn from November to January (Fig. 2a). From October to January, the half-~~  
413 ~~saturation constant for methane decreased from 15 to 2.7  $\mu\text{M}$  for the hypolimnetic assemblage, but increased~~  
414 ~~from 0.7 to 1.2  $\mu\text{M}$  in the epilimnion, with higher  $K_m$  values in November and December (Fig. 2a). A table~~  
415 ~~summarizing the measured methane oxidation kinetics can be found in Supplementary Table 1. The half~~  
416 ~~saturation constants ( $K_m$ ) in the hypolimnion from October to December ( $15.2 \pm 7.1 \mu\text{M}$ ,  $7.1 \pm 2.3 \mu\text{M}$ ,  $6.1 \pm 1.7$~~   
417  ~~$\mu\text{M}$ ) were comparable to  $K_m$  values of hypolimnion samples (one meter above sediment) in two shallow arctic~~  
418 ~~lakes by Lofton et al., (2014). These authors measured values of  $4.45 \pm 2.36 \mu\text{M}$  and  $10.61 \pm 2.03 \mu\text{M}$ . Also in~~  
419 ~~the same range,  $K_m$  values of 5.5  $\mu\text{M}$  and 44  $\mu\text{M}$  were measured in the last meter above the sediment in a boreal~~  
420 ~~lake (Liikanen et al., 2002) and similar values were found for lake sediments (Kuivila et al., 1988; Remsen et al.,~~  
421 ~~1989). In contrast, the epilimnion  $K_m$  in Rotsee in October was  $0.7 \pm 0.5 \mu\text{M}$ , which is far lower than  $K_m$  values~~  
422 ~~measured in previous studies on lacustrine systems, suggesting a well-adapted MOB assemblage with relatively~~  
423 ~~high affinity in the epilimnion. In soils even higher affinities have been measured (0.056–0.186  $\mu\text{M}$ ) (Dunfield~~  
424 ~~et al., 1999) and a high-affinity *Methylocystis* strain has been found to have a  $K_m$  of 0.11  $\mu\text{M}$  (Baani and Liesack,~~  
425 ~~2008). Even when the lake overturn was ongoing in November and December,  $K_m$  values in the epilimnion~~  
426 ~~stayed in the lower range of previously reported  $K_m$  values ( $2.1 \pm 0.9 \mu\text{M}$ ,  $3.3 \pm 0.9 \mu\text{M}$ ), which underlines the~~  
427 ~~adaptation of the MOB assemblage to the continuously lower methane concentrations in the epilimnion.~~

428 The methane affinity of the assemblage in the epilimnion was higher than the methane affinity of the assemblage  
429 in the hypolimnion, which is in line with the methane-deficient conditions in the epilimnion. Previously, starvation  
430 of methane has been shown to decrease the  $K_m$  in *Methylocystis* (Dunfield and Conrad, 2000), but in contrast to  
431 this study we did not observe a constant specific affinity between epi- and hypolimnion, suggesting that indeed  
432 adaptation rather than a starvation response was responsible for the observed low  $K_m$  in the epilimnion. The  
433 pronounced difference in  $K_m$  of the two assemblages in October, when the lake was still stratified, gradually  
434 converged during lake overturn from November to January (Fig. 2a). From October to January, the half-saturation

435 constant for methane decreased from 15 to 2.7  $\mu\text{M}$  for the hypolimnetic assemblage, but increased from 0.7 to 1.2  
436  $\mu\text{M}$  in the epilimnion, with higher  $K_m$  values in November and December (Fig. 2a). A table summarizing the  
437 measured apparent methane oxidation kinetics can be found in Supplementary Tab. 1. The half saturation constants  
438 ( $K_m$ ) in the hypolimnion from October to December ( $15.2 \pm 7.1 \mu\text{M}$ ,  $7.1 \pm 2.3 \mu\text{M}$ ,  $6.1 \pm 1.7 \mu\text{M}$ ) were comparable  
439 to  $K_m$  values of hypolimnion samples (one meter above sediment) in two shallow arctic lakes by Lofton et al.  
440 (2014). These authors measured values of  $4.45 \pm 2.36 \mu\text{M}$  and  $10.61 \pm 2.03 \mu\text{M}$ . Also in the same range,  $K_m$  values  
441 of 5.5  $\mu\text{M}$  and 44  $\mu\text{M}$  were measured in the last meter above the sediment in a boreal lake (Liikanen et al., 2002)  
442 and similar values were found for lake sediments (Kuivila et al., 1988; Remsen et al., 1989). In contrast, the  
443 epilimnion  $K_m$  in Rotsee in October was  $0.7 \pm 0.5 \mu\text{M}$ , which is far lower than  $K_m$  values measured in previous  
444 studies on lacustrine systems, suggesting a well-adapted MOB assemblage with relatively high affinity in the  
445 epilimnion. In soils even higher affinities have been measured (0.056 – 0.186  $\mu\text{M}$ ) (Dunfield et al., 1999) and a  
446 high-affinity *Methylocystis* strain has been found to have a  $K_m$  of 0.11  $\mu\text{M}$  (Baani and Liesack, 2008). Even when  
447 the lake overturn was ongoing in November and December,  $K_m$  values in the epilimnion stayed in the lower range  
448 of previously reported  $K_m$  values ( $2.1 \pm 0.9 \mu\text{M}$ ,  $3.3 \pm 0.9 \mu\text{M}$ ), which underlines the adaptation of the MOB  
449 assemblage to the continuously lower methane concentrations in the epilimnion.

450 We thus concluded that MOB assemblages displayed a specific adaptation to the prevailing methane concentrations  
451 based on the fact that we observed a higher affinity (low  $K_m$ ) in the low-methane epilimnion compared to the  
452 methane rich hypolimnion as long as stratification is present. That the  $K_m$  values of the assemblage in the epilimnion  
453 do not match the *in-situ* methane concentrations is not unexpected: In the mixed layer and under the assumption of  
454 a steady-state, the flux of methane from the hypolimnion is balanced by the methane oxidation rate. Under these  
455 conditions, the *in-situ* methane concentration depends on the half-saturation constant ( $K_m$ ) but should be lower than  
456 it (Supplementary Calculation 1). Per definition, the half-saturation constant is the substrate concentration where  
457 the growth rate is half the maximum growth rate. Even if the growth rate is only half the maximum growth rate,  
458 microbial methane oxidation continues, and methane concentrations decrease to values below  $K_m$ .

459 In contrast to the substrate affinity, the maximum cell-specific methane oxidation rate  $V_{\text{max}}$  started at similar levels  
460 in the stratified lake (Fig. 2b). As methane entered the epilimnion in November, the cell-specific  $V_{\text{max}}$  of the MOB  
461 assemblage in this layer was almost 15 times faster than the hypolimnion assemblage, which ensured a fast methane  
462 oxidation rate in the epilimnion ~~close to the surface during this critical phase. As a consequence, methane~~  
463 ~~concentrations and emissions remain low (Zimmermann et al., 2019) during this critical phase, which has a large~~  
464 ~~potential for methane outgassing to the atmosphere and thus with climate relevance. As a consequence of the high~~  
465 ~~methane oxidation rate, methane concentrations and emissions remain low (Zimmermann et al., 2019).~~ Towards  
466 the end of the lake overturn, when the thermocline had moved to 15 m depth and the two MOB assemblages were  
467 most likely homogenized, methane oxidation rates decreased again. By contrast, the cell-specific methane oxidation  
468 rate in the hypolimnion remained rather constant throughout the overturn from November to December.

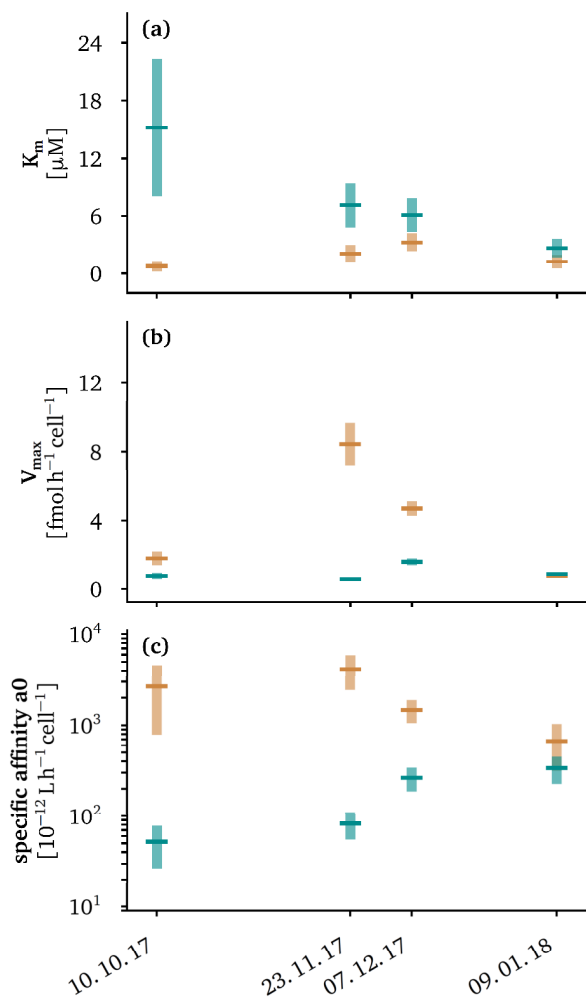


Figure 2. Kinetic properties of the methanotroph assemblage above (orange) and below (cyan) the oxycline for the four sampling campaigns at *in-situ* temperatures of the oxycline. Lines indicate average values; bars represent the 95% confidence interval. We plot 95% confidence intervals as light cyan and light orange vertical bars. Average values are plotted as dark green and dark orange lines. The methane oxidation half-saturation constants ( $K_m$ ) are displayed in panel (a), maximum cell-specific methane oxidation rates in panel (b) and specific affinities, defined as the ratio  $V_{\text{max}}/K_m$ , in panel (c).

The specific affinity ( $V_{\text{max}}/K_m$ ) is the initial slope of the hyperbolic Monod kinetics (Button et al., 2004) and is a pseudo first order rate constant for the methane oxidation rate at limiting methane concentrations. The specific affinity towards methane again suggested that the two communities started out very differently and gradually converged to very similar kinetic properties (Fig. 2c). The convergence of the specific affinity was driven by changes of both,  $K_m$  and  $V_{\text{max}}$  of the MOB assemblage in the epilimnion. The final convergence of the specific affinity of both assemblages is in good agreement with the fact that the two water masses become increasingly similar in terms of substrate availability and temperature towards the end of the lake overturn. The emerging kinetic properties might therefore be the result of a converging succession of the two MOB assemblages. The specific affinity measured for various methanotrophic bacteria are typically in the range of 1 to  $40 \times 10^{-12} \text{L h}^{-1} \text{cell}^{-1}$  (Dunfield and Conrad, 2000; Knief and Dunfield, 2005; Tveit et al., 2019) with a few exceptions where specific affinities of up to  $600 \times 10^{-12} \text{L h}^{-1} \text{cell}^{-1}$  were reported (Calhoun and King, 1997). The specific affinities of  $52$ – $338 \times 10^{-12} \text{L h}^{-1} \text{cell}^{-1}$ , of the MOB assemblage in the hypolimnion were well in the range of these reported values. However, the MOB assemblage in the epilimnion showed much higher specific affinities suggesting that these assemblages were well adapted to the very methane limited conditions in the epilimnion.

Methanotroph cell counts suggest that both the MOB assemblage above and below the oxycline were actively growing over the course of the overturn. The specific affinity ( $V_{\text{max}}/K_m$ ) is the initial slope of the hyperbolic Monod kinetics (Button et al., 2004) and is a pseudo first order rate constant for the methane oxidation rate at limiting methane concentrations. The specific methane affinity of the two communities again started out very differently and gradually converged to very similar kinetic properties (Fig. 2c). The convergence of the specific affinity in the epilimnion and in the hypolimnion was driven by changes of both,  $K_m$  and  $V_{\text{max}}$  of the respective MOB assemblages. The final convergence of the specific affinity of both assemblages is in good agreement with the fact that the two water masses become increasingly similar in terms of substrate availability and temperature towards the end of the lake overturn. The emerging kinetic properties might therefore be the result of a converging succession of the two

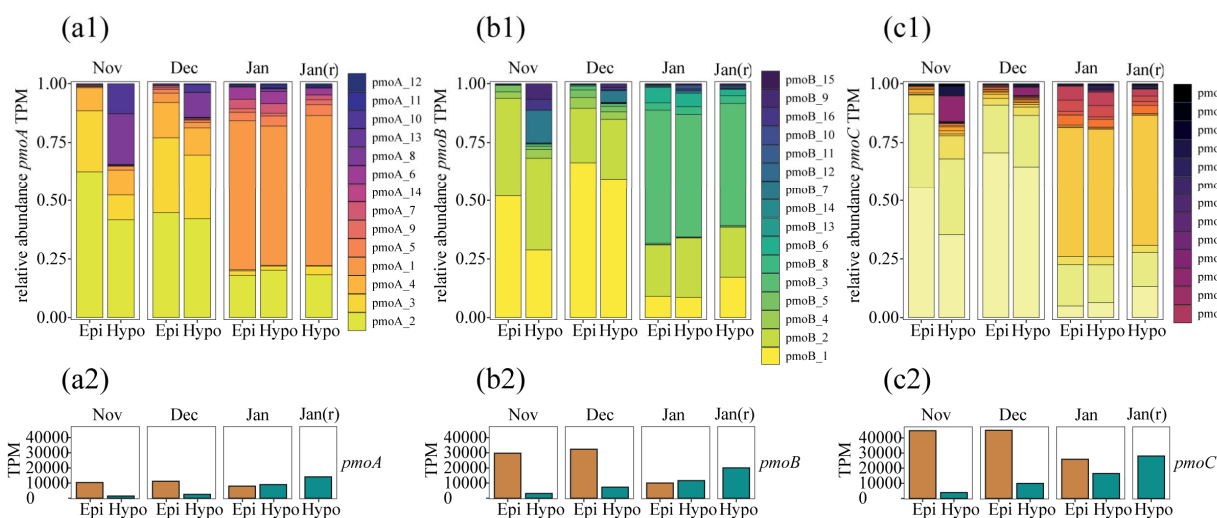
492 MOB assemblages. The *specific affinity* measured for various methanotrophic bacteria are typically in the range of  
 493 1 to  $40 \times 10^{-12} \text{ L h}^{-1} \text{ cell}^{-1}$  (Dunfield and Conrad, 2000; Knief and Dunfield, 2005; Tveit et al., 2019) with a few  
 494 examples where specific affinities of up to  $800 \times 10^{-12} \text{ L h}^{-1} \text{ cell}^{-1}$  were reported (Calhoun and King, 1997; Kolb et  
 495 al., 2005). The specific affinities of  $52 - 338 \times 10^{-12} \text{ L h}^{-1} \text{ cell}^{-1}$ , of the MOB assemblage in the hypolimnion were  
 496 thus well in the range of these reported values. However, the MOB assemblage in the epilimnion showed much  
 497 higher specific affinities suggesting that these assemblages were well adapted to the very methane limited  
 498 conditions in the epilimnion.

499 Methanotroph cell counts suggest that both the MOB assemblage above and below the oxycline were actively  
 500 growing over the course of the overturn (Supplementary Fig. 1). In the epilimnion the abundance of MOB increased  
 501 from  $0.1 \times 10^5$  to  $2 \times 10^5$  cells  $\text{mL}^{-1}$  from October to December, below the oxycline the abundance increased from  
 502  $0.8 \times 10^5$  to  $1.2 \times 10^5$  cells  $\text{mL}^{-1}$ . The *in-situ* methane oxidation rates (Supplementary Table 1) of the MOB assemblage  
 503 in the epilimnion accounted for about 25 % (median) were all below 50 % of the maximum methane oxidation  
 504 rate  $V_{\text{max}}$  from October to December. For the MOB assemblage in the hypolimnion, the *in-situ* methane oxidation  
 505 rates were 93 % (median) all above 67 % of the maximum methane oxidation rate. This  $V_{\text{max}}$ . Even though we don't  
 506 have enough data points to recognize specific trends, the clear differences in the percentage range suggests that the  
 507 growth of the MOB assemblage in the epilimnion was generally methane limited during lake overturn, despite their  
 508 higher methane affinity.

### 509 3.3 Dynamics of the MOB assemblage and variants of pMMO

510 Methane oxidation during lake overturn was performed by diverse assemblages of MOB as determined by  
 511 metatranscriptomic analysis (Fig. 3a1-c1). Thus, the reported kinetics reflect aggregate properties of the  
 512 respective assemblage. In line with previous lake studies (Biderre-Petit et al., 2011; Mayr et al., 2019a; Sundh et  
 513 al., 2005), the majority of *pmoCAB* variants were associated with type Ia MOB (*Gammaproteobacteria*). In  
 514 addition, one variant associated with type Ib MOB (*Gammaproteobacteria*) and up to three variants associated  
 515 with type II MOB (*Alphaproteobacteria*) were found (Supplementary Table 2), but these only showed a low  
 516 abundance and decreasing trend. Evidence for the presence or expression of previously described high affinity  
 517 pMMO (Baani and Liesack, 2008) was not found in the metagenomic or metatranscriptomic dataset. We detected  
 518 sMMO genes (*mmoXYZ*) but transcription was very low (maximum of 6 TPM per sample, Supplementary Table  
 519 3) compared to pMMO. This raises the question under which conditions MOB express sMMO. On the transcript  
 520 and peptide level the expression of this enzyme is often very low or undetectable under environmental conditions  
 521 (Cheema et al., 2015; Dumont et al., 2013; Taubert et al., 2019). Our results suggest that conventional pMMO  
 522 was the main enzyme responsible for methane oxidation under different methane concentrations and  
 523 environmental conditions in the lake water column.

524 Methane oxidation during lake overturn was performed by diverse assemblages of MOB that changed considerably  
 525 over time, as determined by metatranscriptomic analysis (Fig. 3a-c). Thus, the reported apparent kinetics reflect



526 composite properties of the respective assemblage. In line with previous lake studies (Biderre-Petit et al., 2011;

Mayr et al., 2020a; Sundh et al., 2005), the majority of *pmoCAB* variants were associated with type Ia MOB (Fig. 3a, green, *Gammaproteobacteria*). Most of these could not be classified at lower taxonomic levels, but group close to reference sequences from various different genera e.g. *Crenothrix*, *Methylobacter*, *Methylovulum* and Aquatic cluster 5 group (Supplementary Fig. 2). However, one sequence variant could be classified as Lake cluster I which was abundant especially in Nov and Dec (Fig. 3 a, b). In addition, one variant associated with *Methyloparacoccus* (type Ib, *Gammaproteobacteria*) and up to two variants affiliated with type II MOB (*Alphaproteobacteria*) were found (Fig. 3a), the latter showed a low abundance and decreasing trend over time. Evidence for the presence or expression of previously described high affinity pMMO (Baani and Liesack, 2008) was not found in the metagenomic or metatranscriptomic dataset. We detected sMMO genes (*mmoXYZ*) but transcription was very low (maximum of 6 TPM per sample, Supplementary Tab. 2) compared to pMMO. This raises the question under which conditions MOB express sMMO. On the transcript and peptide level the expression of this enzyme is often very low or undetectable under environmental conditions (Cheema et al., 2015; Dumont et al., 2013; Taubert et al., 2019). Our results suggest that conventional pMMO was the main enzyme responsible for methane oxidation under different methane concentrations and environmental conditions in the lake water column.

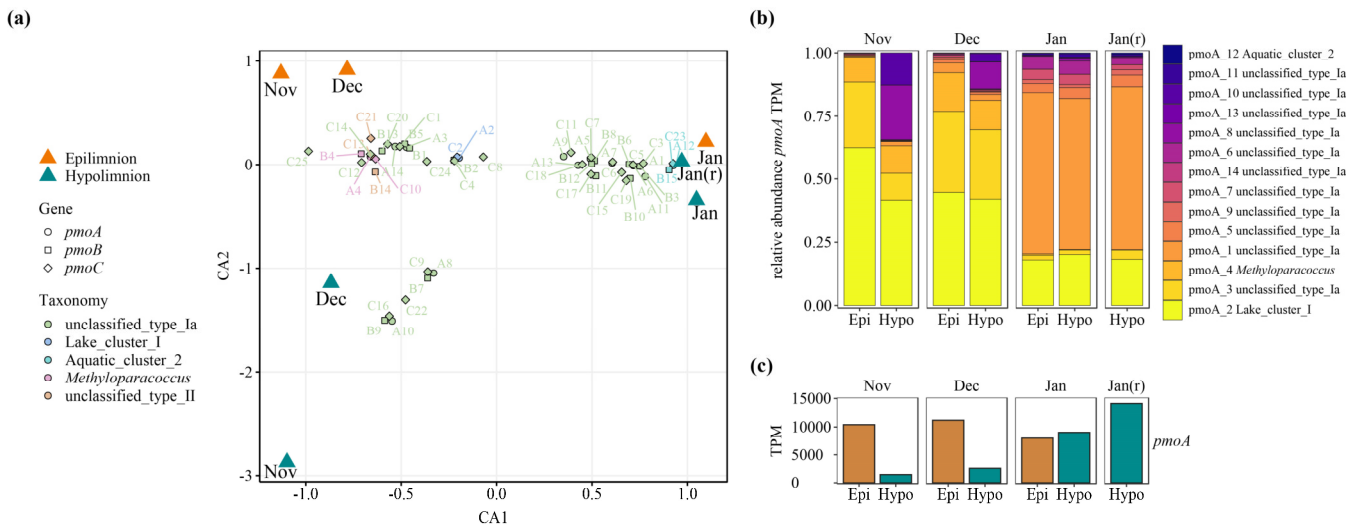


**Figure 3. Transcriptional activity of genes encoding pMMO in November, December and January 2017/2018 during overturn in Rotsee. The January hypolimnion sample was measured twice extracted from two filters and the replicate is labelled as Jan-(r). Relative abundance of gene variants of (a1) *pmoA*, (b1) *pmoB*, (c1) *pmoC* based on transcripts per million (TPM), mapped at 99% identity. *pmoCAB* variants were assembled from metagenomes/metatranscriptomes originating and mapped at 99% identity. The samples originate from the same depths and dates as shown in Fig. 1. Different color schemes were chosen for 1. From October no metatranscriptomes are available. (a) Correspondence analysis (CA) of combined, square root transformed *pmoCAB* TPM (transcripts per million) data. Sample scores are shown as big coloured triangles (orange = epilimnion and cyan = hypolimnion). Sequence variant scores are shown as smaller symbols; circle = *pmoA*, square = *pmoB*, diamond = *pmoC*. Identified variants of each gene are numbered and abbreviated as *pmoA* = A, *pmoB* = B, *pmoC* = C. Colours depict the taxonomic classification of the sequence variants. (a2) based on a phylogenetic tree (Supplementary Fig. 2). (b) Relative abundance of gene variants of *pmoA*, based on transcripts per million (TPM). The corresponding figures for *pmoB*, (b2) and *pmoC* variants are shown in Supplementary Fig. 3. (c) *pmoA* shown as summed TPM of all variants for epi- and hypolimnion (orange and cyan, respectively). Epi = epilimnion, Hypo = hypolimnion. The figures for *pmoB* and *pmoC* are shown in Supplementary Fig. 3.**

In November, and to a lesser degree in December, the composition of transcribed *pmoCAB* gene variants differed between epi- and hypolimnion, with some variants (e.g. *pmoA*\_8 and 10, *pmoB*\_7, 9 and 16, *pmoC*\_9, 16, 22) being confined to the hypolimnion (Fig. 3a1-e1, 3a, b). In November and December the relative transcript abundance of *pmoCAB* was higher in the epilimnion, but the activity in the hypolimnion increased over time and was similar in both depths in January (Fig. 3c, Supplementary Fig. 3c,d). The difference in gene transcription reflects changes in the transcriptionally active MOB assemblage (see detrended correspondence analysis in Supplementary Fig. 2), which, which may explain the observed differences in the apparent methane affinity (Fig. 23a). Notably however, a prominent proportion of the *pmoCAB* gene variants transcribed in the epilimnion were also present in high relative abundance in the hypolimnion, which likely reflects the increasing influence of the highly transcriptionally active epilimnion assemblage (Fig. 3a2-e2, 3b, c, Supplementary Fig. 3) on the hypolimnion assemblage during lake overturn (Mayr et al., 2019b). Thus, a contribution of organisms present

in different physiological states (e.g. starvation) to the difference in apparent kinetics cannot be ruled out by this data. Unfortunately, we do not have lack information on the assemblage for the October sampling where the half saturation constants differed most between epi- and hypolimnion. However, based on observations of the overturn period the year before (Mayr et al., 2019b), (Mayr et al., 2020b), it can be assumed that the two layers harboured distinct MOB assemblages also in October, possibly likely with less species overlap.

The composition of transcribed *pmoCAB* variants showed a distinct change over time (Fig. 3a1-e1 and Supplementary Fig. 2). The relative abundance of the *pmoCAB* variants that were specific to the hypolimnion decreased until January (Fig. 3a1-e1) and the two MOB assemblages became increasingly similar in terms of their kinetic properties (Fig. 2). From December to January another strong shift in the MOB assemblage towards dominance of *pmoA\_1*, *pmoB\_3* and *pmoC\_3* occurred. This did however not change the methane affinity much (Fig. 2), suggesting that different MOB assemblages can have similar methane affinities. The shift of the MOB assemblage was accompanied by a drop in temperature and rise in oxygen, which are probable drivers of MOB succession in addition to methane availability (Hernandez et al., 2015; Oshkin et al., 2015; Trotsenko and Khmelenina, 2005). With this shift, we also observed a decrease in  $V_{max}$  per cell (Fig. 2B). We attribute this to a shift from growth-oriented MOB dominating the bloom phase to a late-successional MOB assemblage adapted to cold temperatures as observed the year before (Mayr et al., 2019b). Further, the metatranscriptomic analysis supports the interpretation that the observed differences in methane oxidation kinetic parameters between water layers and over time have a basis in compositional differences of the transcriptionally active MOB assemblages.

#### 4 Conclusions

Similar to observations made on MOB communities the year before (Mayr et al., 2020b), the *pmoCAB* transcript variants confined to the hypolimnion (e.g. *pmoA\_8*) decreased over time and did not establish in the epilimnion (Fig. 3b, Supplementary Fig. 3c,d). In January the *pmoCAB* composition became almost indistinguishable between epilimnion and hypolimnion (Fig. 3a,b). At the same time their apparent kinetic properties became increasingly similar as well (Fig. 2), which is also in line with the advanced stage of the mixing processes (Fig. 1d). The replicate sample Jan(r) showed a very similar composition providing confidence in the metatranscriptomic analysis, but also showed some variability concerning the summed TPM abundance of the *pmoCAB* variants (Fig. 3c). From December to January a strong shift in the MOB assemblage towards dominance of *pmoA\_1*, *pmoB\_3* and *pmoC\_3* occurred (Fig. 3a, b). The shift of the MOB assemblage was accompanied by a drop in temperature and rise in oxygen, which are probable drivers of MOB succession in addition to methane availability (Hernandez et al., 2015; Oshkin et al., 2015; Trotsenko and Khmelenina, 2005). This did however not lead to much change in the methane affinity (Fig. 2), suggesting that different MOB assemblages can have similar methane affinities. Nevertheless, we hypothesize that the composition of *pmoCAB* rather than the summed TPM may be important for explaining the kinetic properties. With this shift, we also observed a decrease in  $V_{max}$  per cell (Fig. 2b). In agreement with observations made the year before (Mayr et al., 2020b), we attribute the decrease in  $V_{max}$  per cell to a shift from growth-oriented MOB dominating the bloom phase to a late-successional MOB assemblage adapted to cold temperatures. Overall, the metatranscriptomic analysis supports the hypothesis that the observed differences in apparent methane oxidation kinetic parameters between water layers and over time have a basis in compositional differences of the transcriptionally active MOB assemblages.

#### 4 Conclusions

In Lake Rotsee, as in many other stratified lakes, (Bastviken et al., 2004; Borrel et al., 2011), the high methane availability in the hypolimnion contrasts with low methane availability in the epilimnion. Therefore, we hypothesized that the resident MOB assemblages are adapted to the respective local conditions. Our field study revealed a high level of adaptation of the MOB assemblage: the  $K_m$  differed by two orders of magnitude between epi- and was 20 times higher in the hypolimnion than in the epilimnion during stable stratification. Transcribed methane oxidation genes differed as well, indicating that methane affinity is an important trait structuring MOB assemblages in this system. The MOB assemblage and its apparent kinetic traits parameters adapted rapidly to changing conditions in the epilimnion. In October, the low epilimnion  $K_m$  suggested an adaptation to oligotrophie

601 ~~conditions with~~ low methane concentrations. During the autumn overturn, *affinity* decreased slightly but remained  
602 ~~below~~ hypolimnion values, reflecting persistently low methane concentrations that suggest methane-limited  
603 growth despite higher methane input. We observed increased  $V_{\max}$  in the epilimnion during November and  
604 December. ~~In ensuring a fast methane oxidation rate in~~ this period, ~~with~~ continuous transport of methane into the  
605 epilimnion ~~provided an advantage of fast-growing MOB over slower competitors~~. By contrast, in the hypolimnion  
606 methane concentrations during overturn exceeded the  $K_m$  several-fold suggesting that MOB growth was not limited  
607 by methane concentrations.

608 Our transcriptomic analysis revealed that the variations in methane *affinity* were ~~entirely~~ linked to ~~transcribed, and~~  
609 ~~thus likely expressed, *pmoCAB* variants~~ ~~and~~. We also found that pMMO appeared to be the dominant methane  
610 monooxygenase throughout. ~~We and~~ found no evidence for shifts between sMMO and pMMO transcription as  
611 hypothesized previously (Semrau et al., 2018) ~~nor~~ (Semrau et al., 2018). ~~Nor~~ could we observe ~~any of the~~ previously  
612 described high-*affinity* pMMO variants, which suggests considerable, so far unappreciated variability in ~~apparent~~  
613 pMMO kinetics. Further research will be needed to obtain kinetic data on individual pMMO variants. ~~However,~~  
614 ~~the provided~~ ~~and to better understand the physiological basis of the apparent methane oxidation kinetics. The~~  
615 ~~provided apparent~~ kinetic parameters for lake MOB assemblages will inform future trait or process-based models  
616 of the MOB assemblage and methane emissions. In summary, our work demonstrates that differential methane  
617 availability governed by lake mixing regimes ~~creates~~ niches for MOB assemblages with well-adapted  
618 methane-oxidation kinetics. ~~in Lake Rotsee, a mechanism that possibly applies to many seasonally stratified lakes~~  
619 ~~in which vertical structure and temporal succession of MOB may be similar.~~

## 620 Figure captions

621 Figure 1. Substrate concentrations and **apparent** methane oxidation ~~rates~~**kinetics** during lake overturn in **Lake Rotsee**. (a - d)  
622 Oxygen concentration **and temperature** profiles during the four field campaigns at the dates indicated. The sampling depths above  
623 (orange) and below (cyan) the oxycline are indicated by ~~arrows~~**a horizontal bar**. Numbers next to the ~~arrows~~**bars** represent  
624 methane concentrations in  $\mu\text{M}$  at the respective depths. (e - h) Cell-specific methane oxidation rates (MOX) of water samples  
625 incubated with different methane concentrations. Lines indicate least-square fits of the Monod kinetics. For each campaign, we  
626 incubated samples from both depths close to *in-situ* temperature ~~(indicated in bold, given next to the annotation (incub. =~~  
627 **incubated)**.

628  
629 Figure 2. ~~Kinetic~~**Apparent kinetic** properties of the methanotroph assemblage above (orange) and below (cyan) the oxycline for the  
630 four sampling campaigns at *in-situ* temperatures of the oxycline. ~~Lines indicate average values; bars represent the 95%~~  
631 ~~confidence interval. We plot 95% confidence intervals as light cyan and light orange vertical bars. Average values are plotted as~~  
632 ~~dark green and dark orange lines~~. The methane oxidation half-saturation constants ( $K_m$ ) are displayed in panel (a), maximum cell-  
633 specific methane oxidation rates in panel (b) and specific affinities, defined as the ratio  $V_{\max}/K_m$ , in panel (c).

634  
635 Figure 3. ~~Transcriptional activity of genes~~**Transcribed gene variants** encoding pMMO in November, December and January  
636 2017/2018 during overturn in Rotsee. The January hypolimnion sample was ~~measured twice~~**extracted from two filters** and the  
637 replicate is labelled as Jan-(r). ~~Relative abundance of gene variants of (a1) pmoA, (b1) pmoB, (c1) pmoC based on~~  
638 ~~transcripts per million (TPM), mapped at 99% identity. pmoCAB variants were assembled from~~  
639 ~~metagenomes~~**metagenomic** and ~~metatranscriptomes~~**metatranscriptomic** samples ~~originating and mapped at 99% identity.~~  
640 ~~The samples originate~~ from the same depths and dates as shown in Fig. 1. ~~Different color schemes were chosen for pmoA,~~  
641 ~~pmoB and pmoC~~. 1. From October no metatranscriptomes are available. (a) Correspondence analysis (CA) of combined, square  
642 root transformed *pmoCAB* TPM (transcripts per million) data. Sample scores are shown as big coloured triangles (orange =  
643 epilimnion and cyan = hypolimnion). Sequence variant scores are shown as smaller symbols; circle = *pmoA*, square = *pmoB*, diamond  
644 = *pmoC*. Identified variants ~~(a2)~~ of each gene are numbered and abbreviated as *pmoA* = A, *pmoB* = B, *pmoC* = C. Colors depict  
645 the taxonomic classification of the sequence variants based on a phylogenetic tree (Supplementary Fig. 2). (b) Relative abundance  
646 of gene variants of *pmoA*, ~~(b2)~~ based on transcripts per million (TPM). The corresponding figures for *pmoB*, ~~(c2)~~ *pmoC* and  
647 *pmoC* variants are shown in Supplementary Fig. 3. (c) *pmoA* shown as summed TPM of all variants for epi- and hypolimnion (orange  
648 and cyan, respectively). Epi = epilimnion, Hypo = hypolimnion. ~~The figures for pmoB and pmoC are shown in Supplementary Fig.~~  
649 ~~3.~~

## 650 Data availability

651 Raw reads of the sequencing project were submitted to the European Nucleotide Archive under project number  
652 PRJEB35558. Methane concentrations, scintillation counts, methane oxidation rates, estimated kinetic parameters  
653 and the identified nucleotide sequences encoding MMO are available at the EAWAG repository under  
654 <https://doi.org/10.25678/0001fa> (Mayr et al., 2019e). <https://doi.org/10.25678/0001fa> (Mayr et al., 2019).

## 655 Author contribution

656 MJM and MZ contributed equally to this work. MJM, MZ, and HB conceptualized the study and MJM, MZ and  
657 JD carried out the investigation. MJM and MZ curated, ~~analyzed~~**analysed** and visualized the data. MJM and MZ  
658 wrote the original draft of the manuscript with contributions from BW, HB and JD. Funding was acquired by HB.

## 659 Competing interests

660 The authors declare that they have no conflict of interest.

## 661 **Acknowledgements**

662 This research was funded by the Swiss National Science Foundation (grant CR23I3\_156759), by ETH Zurich and  
663 Eawag. We are grateful to Andreas Brand for his support and advice in the early stages of the project, to Carsten  
664 Schubert, Serge Robert and Daniel Steiner for the possibility and the support to use the equipment for radioisotope  
665 and methane measurement. We are also grateful to Lea Steinle for sharing her expertise on how to handle the  
666 ~~radiolabeled~~radiolabelled methane. We would like to thank Karin Beck and Patrick Kathriner for technical  
667 assistance during field work and laboratory analysis. We thank Feng Ju and Robert Niederdorfer for advice on the  
668 bioinformatics analysis. Sequencing data were ~~analyzed~~analysed in collaboration with the Genetic Diversity Centre  
669 (GDC) of ETH Zurich.

- 671 Baani, M. and Liesack, W.: Two isozymes of particulate methane monooxygenase with different methane  
672 oxidation kinetics are found in *Methylocystis* sp. strain SC2., *Proc. Natl. Acad. Sci. U. S. A.*, 105(29), 10203–8,  
673 doi:10.1073/pnas.0702643105, 2008.
- 674 Bastviken, D., Ejlertsson, J. and Tranvik, L.: Measurement of methane oxidation in lakes: A comparison of  
675 methods, *Environ. Sci. Technol.*, 36(15), 3354–3361, doi:10.1021/es010311p, 2002.
- 676 Biderre-Petit, C., Jézéquel, D., Dugat-Bony, E., Lopes, F., Kuever, J., Borrel, G., Viollier, E., Fonty, G. and  
677 Peyret, P.: Identification of microbial communities involved in the methane cycle of a freshwater meromictic  
678 lake, *FEMS Microbiol. Ecol.*, 77(3), 533–545, doi:10.1111/j.1574-6941.2011.01134.x, 2011.
- 679 Bolger, A. M., Lohse, M. and Usadel, B.: Trimmomatic: A flexible trimmer for Illumina sequence data,  
680 *Bioinformatics*, 30(15), 2114–2120, doi:10.1093/bioinformatics/btu170, 2014.
- 681 Brand, A., Bruderer, H., Oswald, K., Guggenheim, C., Schubert, C. J. and Wehrli, B.: Oxygenic primary  
682 production below the oxycline and its importance for redox dynamics, *Aquat. Sci.*, 78(4), 727–741,  
683 doi:10.1007/s00027-016-0465-4, 2016.
- 684 Buchfink, B., Xie, C. and Huson, D. H.: Fast and sensitive protein alignment using DIAMOND, *Nat. Methods*,  
685 12(1), 59–60, doi:10.1038/nmeth.3176, 2014.
- 686 Bushnell, B.: BBMap: a fast, accurate, splice-aware aligner., 2014.
- 687 Bussmann, I., Matousu, A., Osudar, R. and Mau, S.: Assessment of the radio-<sup>3</sup>H-CH<sub>4</sub> tracer technique to measure  
688 aerobic methane oxidation in the water column, *Limnol. Oceanogr. Methods*, 13(6), 312–327,  
689 doi:10.1002/lom3.10027, 2015.
- 690 Button, D. K., Robertson, B., Gustafson, E. and Zhao, X.: Experimental and Theoretical Bases of Specific  
691 Affinity, a Cytoarchitecture Based Formulation of Nutrient Collection Proposed To Supersede the Michaelis-  
692 Menten Paradigm of Microbial Kinetics, *Appl. Environ. Microbiol.*, 70(9), 5511–5521,  
693 doi:10.1128/AEM.70.9.5511-5521.2004, 2004.
- 694 Calhoun, A. and King, G. M.: Regulation of root-associated methanotrophy by oxygen availability in the  
695 rhizosphere of two aquatic macrophytes, *Appl. Environ. Microbiol.*, 63(8), 3051–3058,  
696 doi:10.1029/2012WR012444, 1997.
- 697 Cheema, S., Zeyer, J. and Henneberger, R.: Methanotrophic and methanogenic communities in swiss alpine fens  
698 dominated by *Carex rostrata* and *Eriophorum angustifolium*, *Appl. Environ. Microbiol.*, 81(17), 5832–5844,  
699 doi:10.1128/AEM.01519-15, 2015.
- 700 Conrad, R.: The global methane cycle: Recent advances in understanding the microbial processes involved,  
701 *Environ. Microbiol. Rep.*, 1(5), 285–292, doi:10.1111/j.1758-2229.2009.00038.x, 2009.
- 702 Daims, H.: Use of fluorescence in situ hybridization and the daime image analysis program for the cultivation-  
703 independent quantification of microorganisms in environmental and medical samples, *Cold Spring Harb. Protoc.*,  
704 2009(7), db.prot5253, 2009.
- 705 Dam, B., Dam, S., Kube, M., Reinhardt, R. and Liesack, W.: Complete genome sequence of *Methylocystis* sp.  
706 strain SC2, an aerobic methanotroph with high affinity methane oxidation potential, *J. Bacteriol.*, 194(21), 6008–  
707 6009, doi:10.1128/JB.01446-12, 2012.
- 708 DelSontro, T., Beaulieu, J. J. and Downing, J. A.: Greenhouse gas emissions from lakes and impoundments:  
709 Upscaling in the face of global change, *Limnol. Oceanogr. Lett.*, 3(3), 64–75, doi:10.1002/lol2.10073, 2018.
- 710 Dumont, M. G., Pommerenke, B. and Casper, P.: Using stable isotope probing to obtain a targeted  
711 metatranscriptome of aerobic methanotrophs in lake sediment, *Environ. Microbiol. Rep.*, 5(5), 757–764,  
712 doi:10.1111/1758-2229.12078, 2013.
- 713 Dunfield, P. F. and Conrad, R.: Starvation alters the apparent half saturation constant for methane in the type II  
714 methanotroph *Methylocystis* strain LR1, *Appl. Environ. Microbiol.*, 66(9), 4136–4138,

715 doi:10.1128/AEM.66.9.4136-4138.2000, 2000.

716 Dunfield, P. F., Liesack, W., Henckel, T., Knowles, R. and Conrad, R.: High-affinity methane oxidation by a soil  
717 enrichment culture containing a type II methanotroph, *Appl. Environ. Microbiol.*, 65(3), 1009–1014,  
718 doi:10.3109/17435390.2011.562327, 1999.

719 Eller, G., Stubner, S. and Frenzel, P.: Group-specific 16S rRNA targeted probes for the detection of type I and  
720 type II methanotrophs by fluorescence in situ hybridisation, *FEMS Microbiol. Lett.*, 198(2), 91–97,  
721 doi:10.1016/S0378-1097(01)00130-6, 2001.

722 Graf, J. S., Mayr, M. J., Marchant, H. K., Tienken, D., Hach, P. F., Brand, A., Schubert, C. J., Kuypers, M. M. M.  
723 and Milucka, J.: Bloom of a denitrifying methanotroph, ‘*Candidatus Methyloirabilis limnetica*’, in a deep  
724 stratified lake, *Environ. Microbiol.*, 20(7), 2598–2614, doi:10.1111/1462-2920.14285, 2018.

725 Guggenheim, C., Brand, A., Bürgmann, H., Sigg, L. and Wehrli, B.: Aerobic methane oxidation under copper  
726 scarcity in a stratified lake, *Sci. Rep.*, 9(1), 1–11, doi:10.1038/s41598-019-40642-2, 2019.

727 Hanson, R. S. and Hanson, T. E.: Methanotrophic bacteria, *Microbiol. Rev.*, 60(2), 439–471,  
728 doi:10.1002/0471263397.env316, 1996.

729 Hernandez, M. E., Beck, D. A. C., Lidstrom, M. E. and Chistoserdova, L.: Oxygen availability is a major factor  
730 in determining the composition of microbial communities involved in methane oxidation., *PeerJ*, 3(e801), 1–13,  
731 doi:10.7717/peerj.801, 2015.

732 Hyatt, D., Chen, G. L., LoCasio, P. F., Land, M. L., Larimer, F. W. and Hauser, L. J.: Prodigal: prokaryotic  
733 gene recognition and translation initiation site identification, *BMC Bioinformatics*, 11(119), 1–11,  
734 doi:10.3389/fgene.2015.00348, 2010.

735 Kankaala, P., Taipale, S., Nykänen, H. and Jones, R. I.: Oxidation, efflux, and isotopic fractionation of methane  
736 during autumnal turnover in a polyhumic, boreal lake, *J. Geophys. Res. Biogeosciences*, 112(2), 1–7,  
737 doi:10.1029/2006JG000336, 2007.

738 Kirf, M. K., Dinkel, C., Schubert, C. J. and Wehrli, B.: Submicromolar oxygen profiles at the oxic-anoxic  
739 boundary of temperate lakes, *Aquat. Geochemistry*, 20(1), 39–57, doi:10.1007/s10498-013-9206-7, 2014.

740 Knief, C. and Dunfield, P. F.: Response and adaptation of different methanotrophic bacteria to low methane  
741 mixing ratios, *Environ. Microbiol.*, 7(9), 1307–1317, doi:10.1111/j.1462-2920.2005.00814.x, 2005.

742 Kojima, H., Iwata, T. and Fukui, M.: DNA-based analysis of planktonic methanotrophs in a stratified lake,  
743 *Freshw. Biol.*, 54(7), 1501–1509, doi:10.1111/j.1365-2427.2009.02199.x, 2009.

744 Kopylova, E., Noé, L. and Touzet, H.: SortMeRNA: Fast and accurate filtering of ribosomal RNAs in  
745 metatranscriptomic data, *Bioinformatics*, 28(24), 3211–3217, doi:10.1093/bioinformatics/bts611, 2012.

746 Kuivila, K. M., Murray, J. W., Devol, A. H., Lidstrom, M. E. and Reimers, C. E.: Methane cycling in the  
747 sediments of Lake Washington, *Limnol. Oceanogr.*, 33(4), 571–581, doi:10.4319/lo.1988.33.4.0571, 1988.

748 Li, D., Liu, C. M., Luo, R., Sadakane, K. and Lam, T. W.: MEGAHIT: An ultra-fast single-node solution for  
749 large and complex metagenomics assembly via succinct de Bruijn graph, *Bioinformatics*, 31(10), 1674–1676,  
750 doi:10.1093/bioinformatics/btv033, 2015.

751 Li, H., Handsaker, B., Wysoker, A., Fennell, T., Ruan, J., Homer, N., Marth, G., Abecasis, G. and Durbin, R.:  
752 The Sequence Alignment/Map format and SAMtools, *Bioinformatics*, 25(16), 2078–2079,  
753 doi:10.1093/bioinformatics/btp352, 2009.

754 Li, W. and Godzik, A.: Cd-hit: A fast program for clustering and comparing large sets of protein or nucleotide  
755 sequences, *Bioinformatics*, 22(13), 1658–1659, doi:10.1093/bioinformatics/btl158, 2006.

756 Liao, Y., Smyth, G. K. and Shi, W.: FeatureCounts: An efficient general purpose program for assigning sequence  
757 reads to genomic features, *Bioinformatics*, 30(7), 923–930, doi:10.1093/bioinformatics/btt656, 2014.

758 Liikanen, A., Huttunen, J. T., Valli, K. and Martikainen, P. J.: Methane cycling in the sediment and water column  
759 of mid-boreal hyper-eutrophic Lake Kevätön, Finland, *Fundam. Appl. Limnol.*, 154(4), 585–603,

760 [doi:10.1127/archiv-hydrobiol/154/2002/585](https://doi.org/10.1127/archiv-hydrobiol/154/2002/585), 2002.

761 Lofton, D. D., Whalen, S. C. and Hershey, A. E.: Effect of temperature on methane dynamics and evaluation of  
762 methane oxidation kinetics in shallow Arctic Alaskan lakes, *Hydrobiologia*, 721(1), 209–222,  
763 [doi:10.1007/s10750-013-1663-x](https://doi.org/10.1007/s10750-013-1663-x), 2014.

764 Mayr, M. J., Zimmermann, M., Guggenheim, C., Brand, A. and Bürgmann, H.: Niche partitioning of methane-  
765 oxidizing bacteria along the oxygen–methane counter gradient of stratified lakes, *ISME J.*, [doi:10.1038/s41396-019-0515-8](https://doi.org/10.1038/s41396-019-0515-8), 2019a.

766  
767 Mayr, M. J., Zimmermann, M., Dey, J., Brand, A. and Bürgmann, H.: Growth and rapid succession of  
768 methanotrophs effectively limit methane release during lake overturn, *bioRxiv*,  
769 [doi:https://doi.org/10.1101/707836](https://doi.org/10.1101/707836), 2019b.

770 Mayr, M. J., Zimmermann, M., Dey, J., Wehrli, B. and Bürgmann, H.: Data for: Community methane oxidation  
771 kinetics selected by lake mixing regime [Data set], Eawag Swiss Fed. Inst. Aquat. Sci. Technol.,  
772 [doi:10.25678/0001fa](https://doi.org/10.25678/0001fa), 2019c.

773 O’Leary, N. A., Wright, M. W., Brister, J. R., Ciufu, S., Haddad, D., McVeigh, R., Rajput, B., Robbertse, B.,  
774 Smith-White, B., Ako-Adjei, D., Astashyn, A., Badretdin, A., Bao, Y., Blinkova, O., Brover, V., Chetvernin, V.,  
775 Choi, J., Cox, E., Ermolaeva, O., Farrell, C. M., Goldfarb, T., Gupta, T., Haft, D., Hateher, E., Hlavina, W.,  
776 Joardar, V. S., Kodali, V. K., Li, W., Maglott, D., Masterson, P., McGarvey, K. M., Murphy, M. R., O’Neill, K.,  
777 Pujar, S., Rangwala, S. H., Rausch, D., Riddick, L. D., Schoch, C., Shkeda, A., Storz, S. S., Sun, H., Thibaud-  
778 Nissen, F., Tolstoy, I., Tully, R. E., Vatsan, A. R., Wallin, C., Webb, D., Wu, W., Landrum, M. J., Kimchi, A.,  
779 Tatusova, T., DiCuccio, M., Kitts, P., Murphy, T. D. and Pruitt, K. D.: Reference sequence (RefSeq) database at  
780 NCBI: Current status, taxonomic expansion, and functional annotation, *Nucleic Acids Res.*, 44(D1), D733–D745,  
781 [doi:10.1093/nar/gkv1189](https://doi.org/10.1093/nar/gkv1189), 2016.

782 Oshkin, I. Y., Beck, D. A. C., Lamb, A. E., Tehesnokova, V., Benuska, G., Metagart, T. L., Kalyuzhnaya, M.  
783 G., Dedysh, S. N., Lidstrom, M. E. and Chistoserdova, L.: Methane fed microbial microcosms show differential  
784 community dynamics and pinpoint taxa involved in communal response, *ISME J.*, 9(5), 1119–1129,  
785 [doi:10.1038/ismej.2014.203](https://doi.org/10.1038/ismej.2014.203), 2015.

786 Oswald, K., Milucka, J., Brand, A., Littmann, S., Wehrli, B., Kuypers, M. M. M. and Schubert, C. J.: Light-  
787 dependent aerobic methane oxidation reduces methane emissions from seasonally stratified lakes, *PLoS One*,  
788 10(7), 1–22, [doi:10.1371/journal.pone.0132574](https://doi.org/10.1371/journal.pone.0132574), 2015.

789 Pernthaler, A., Pernthaler, J. and Amann, R.: Fluorescence In Situ Hybridization and Catalyzed Reporter  
790 Deposition for the Identification of Marine Bacteria, *Appl. Environ. Microbiol.*, 68(6), 3094–3101,  
791 [doi:10.1128/AEM.68.6.3094](https://doi.org/10.1128/AEM.68.6.3094), 2002.

792 Remsen, C. C., Minnich, E. C., Stephens, R. S., Buchholz, L. and Lidstrom, M. E.: Methane Oxidation in Lake  
793 Superior Sediments, *J. Great Lakes Res.*, 15(1), 141–146, [doi:10.1016/S0380-1330\(89\)71468-4](https://doi.org/10.1016/S0380-1330(89)71468-4), 1989.

794 Schmieder, R. and Edwards, R.: Quality control and preprocessing of metagenomic datasets, *Bioinformatics*,  
795 27(6), 863–864, [doi:10.1093/bioinformatics/btr026](https://doi.org/10.1093/bioinformatics/btr026), 2011.

796 Schubert, C. J., Diem, T. and Eugster, W.: Methane emissions from a small wind shielded lake determined by  
797 eddy covariance, flux chambers, anchored funnels, and boundary model calculations: A comparison, *Environ.  
798 Sci. Technol.*, 46(8), 4515–4522, [doi:10.1021/es203465x](https://doi.org/10.1021/es203465x), 2012.

799 Seemann, T.: Prokka: Rapid prokaryotic genome annotation, *Bioinformatics*, 30(14), 2068–2069,  
800 [doi:10.1093/bioinformatics/btu153](https://doi.org/10.1093/bioinformatics/btu153), 2014.

801 Semrau, J. D., DiSpirito, A. A., Gu, W. and Yoon, S.: Metals and methanotrophy, *Appl. Environ. Microbiol.*,  
802 84(6), 7–14, [doi:10.1128/AEM.02289-17](https://doi.org/10.1128/AEM.02289-17), 2018.

803 Shen, W., Le, S., Li, Y. and Hu, F.: SeqKit: A cross-platform and ultrafast toolkit for FASTA/Q file  
804 manipulation, *PLoS One*, 11(10), 1–10, [doi:10.1371/journal.pone.0163962](https://doi.org/10.1371/journal.pone.0163962), 2016.

805 Steinle, L., Graves, C. A., Treude, T., Ferré, B., Biastoch, A., Bussmann, I., Berndt, C., Krastel, S., James, R. H.,  
806 Behrens, E., Böning, C. W., Greinert, J., Sapart, C. J., Scheinert, M., Sommer, S., Lehmann, M. F. and Niemann,

807 [H.: Water column methanotrophy controlled by a rapid oceanographic switch, \*Nat. Geosci.\*, 8\(5\), 378–382,](#)  
808 [doi:10.1038/ngeo2420, 2015.](#)

809 [Steinsberger, T., Schmid, M., Wüest, A., Schwefel, R., Wehrli, B. and Müller, B.: Organic carbon mass](#)  
810 [accumulation rate regulates the flux of reduced substances from the sediments of deep lakes, \*Biogeosciences\*,](#)  
811 [14\(13\), 3275–3285, doi:10.5194/bg-14-3275-2017, 2017.](#)

812 [Stuart, A. and Ord, J. K.: Kendall's Advanced Theory of Statistics: Volume 1: Distribution Theory, Wiley., 2009.](#)

813 [Sundh, I., Bastviken, D. and Tranvik, L. J.: Abundance, activity, and community structure of pelagic methane-](#)  
814 [oxidizing bacteria in temperate lakes, \*Appl. Environ. Microbiol.\*, 71\(11\), 6746–6752,](#)  
815 [doi:10.1128/AEM.71.11.6746-6752.2005, 2005.](#)

816 [Taubert, M., Grob, C., Crombie, A., Howat, A. M., Burns, O. J., Weber, M., Lott, C., Kaster, A., Vollmers, J.,](#)  
817 [Jehmlich, N., von Bergen, M., Chen, Y. and Murrell, J. C.: Communal metabolism by Methyloceceae and](#)  
818 [Methylophilaceae is driving rapid aerobic methane oxidation in sediments of a shallow seep near Elba, Italy,](#)  
819 [\*Environ. Microbiol.\*, 00, doi:10.1111/1462-2920.14728, 2019.](#)

820 [Trotsenko, Y. A. and Khmelena, V. N.: Aerobic methanotrophic bacteria of cold ecosystems, \*FEMS Microbiol.\*](#)  
821 [\*Ecol.\*, 53\(1\), 15–26, doi:10.1016/j.femsec.2005.02.010, 2005.](#)

822 [Tveit, A. T., Hestnes, A. G., Robinson, S. L., Schintlmeister, A., Dedysh, S. N., Jehmlich, N., Von Bergen, M.,](#)  
823 [Herbold, C., Wagner, M., Richter, A. and Svenning, M. M.: Widespread soil bacterium that oxidizes atmospheric](#)  
824 [methane, \*Proc. Natl. Acad. Sci. U. S. A.\*, 116\(17\), 8515–8524, doi:10.1073/pnas.1817812116, 2019.](#)

825 [Wagner, G. P., Kin, K. and Lynch, V. J.: Measurement of mRNA abundance using RNA-seq data: RPKM](#)  
826 [measure is inconsistent among samples, \*Theory Biosci.\*, 131\(4\), 281–285, doi:10.1007/s12064-012-0162-3, 2012.](#)

827 [Wiesenburg, D. A. and Guinasso, N. L.: Equilibrium solubilities of methane, carbon monoxide, and hydrogen in](#)  
828 [water and sea water, \*J. Chem. Eng. Data\*, 24\(4\), 356–360, doi:10.1021/jc60083a006, 1979.](#)

829 [Zimmermann, M., Mayr, M. J., Bouffard, D., Eugster, W., Steinsberger, T., Wehrli, B., Brand, A. and Bürgmann,](#)  
830 [H.: Lake overturn as a key driver for methane oxidation, \*bioRxiv\*, 689182, doi:10.1101/689182, 2019.](#)

831 [Baani, M. and Liesack, W.: Two isozymes of particulate methane monooxygenase with different methane](#)  
832 [oxidation kinetics are found in \*Methylocystis\* sp. strain SC2., \*Proc. Natl. Acad. Sci. U. S. A.\*, 105\(29\), 10203–8,](#)  
833 [doi:10.1073/pnas.0702643105, 2008.](#)

834 [Bastviken, D., Cole, J., Pace, M. and Tranvik, L.: Methane emissions from lakes: Dependence of lake](#)  
835 [characteristics, two regional assessments, and a global estimate, \*Global Biogeochem. Cycles\*, 18\(4\), 1–12,](#)  
836 [doi:10.1029/2004GB002238, 2004.](#)

837 [Bastviken, D., Ejlertsson, J. and Tranvik, L.: Measurement of methane oxidation in lakes: A comparison of](#)  
838 [methods, \*Environ. Sci. Technol.\*, 36\(15\), 3354–3361, doi:10.1021/es010311p, 2002.](#)

839 [Biderre-Petit, C., Jézéquel, D., Dugat-Bony, E., Lopes, F., Kuever, J., Borrel, G., Viollier, E., Fonty, G. and](#)  
840 [Peyret, P.: Identification of microbial communities involved in the methane cycle of a freshwater meromictic](#)  
841 [lake, \*FEMS Microbiol. Ecol.\*, 77\(3\), 533–545, doi:10.1111/j.1574-6941.2011.01134.x, 2011.](#)

842 [Boehrer, B. and Schultze, M.: Stratification of lakes, \*Rev. Geophys.\*, 46\(2\), 1–27, doi:10.1029/2006RG000210,](#)  
843 [2008.](#)

844 [Bolger, A. M., Lohse, M. and Usadel, B.: Trimmomatic: A flexible trimmer for Illumina sequence data,](#)  
845 [\*Bioinformatics\*, 30\(15\), 2114–2120, doi:10.1093/bioinformatics/btu170, 2014.](#)

846 [Borrel, G., Jézéquel, D., Biderre-Petit, C., Morel-Desrosiers, N., Morel, J. P., Peyret, P., Fonty, G. and Lehours,](#)  
847 [A. C.: Production and consumption of methane in freshwater lake ecosystems, \*Res. Microbiol.\*, 162\(9\), 833–847,](#)  
848 [doi:10.1016/j.resmic.2011.06.004, 2011.](#)

849 [Brand, A., Bruderer, H., Oswald, K., Guggenheim, C., Schubert, C. J. and Wehrli, B.: Oxygenic primary](#)  
850 [production below the oxycline and its importance for redox dynamics, \*Aquat. Sci.\*, 78\(4\), 727–741,](#)  
851 [doi:10.1007/s00027-016-0465-4, 2016.](#)

852 [Buchfink, B., Xie, C. and Huson, D. H.: Fast and sensitive protein alignment using DIAMOND, Nat. Methods,](#)  
853 [12\(1\), 59–60, doi:10.1038/nmeth.3176, 2014.](#)

854 [Bushnell, B.: BBMap: a fast, accurate, splice-aware aligner. \[online\] Available from:](#)  
855 <https://escholarship.org/uc/item/1h3515gn>, 2014.

856 [Bussmann, I., Matousu, A., Osudar, R. and Mau, S.: Assessment of the radio 3H-CH4 tracer technique to](#)  
857 [measure aerobic methane oxidation in the water column, Limnol. Oceanogr. Methods, 13\(6\), 312–327,](#)  
858 [doi:10.1002/lom3.10027, 2015.](#)

859 [Button, D. K., Robertson, B., Gustafson, E. and Zhao, X.: Experimental and theoretical bases of specific affinity,](#)  
860 [a cytoarchitecture-based formulation of nutrient collection proposed to supercede the Michaelis-Menten](#)  
861 [paradigm of microbial kinetics, Appl. Environ. Microbiol., 70\(9\), 5511–5521, doi:10.1128/AEM.70.9.5511-](#)  
862 [5521.2004, 2004.](#)

863 [Calhoun, A. and King, G. M.: Regulation of root-associated methanotrophy by oxygen availability in the](#)  
864 [rhizosphere of two aquatic macrophytes, Appl. Environ. Microbiol., 63\(8\), 3051–3058,](#)  
865 [doi:10.1029/2012WR012444, 1997.](#)

866 [Cheema, S., Zeyer, J. and Henneberger, R.: Methanotrophic and methanogenic communities in swiss alpine fens](#)  
867 [dominated by Carex rostrata and Eriophorum angustifolium, Appl. Environ. Microbiol., 81\(17\), 5832–5844,](#)  
868 [doi:10.1128/AEM.01519-15, 2015.](#)

869 [Conrad, R.: The global methane cycle: Recent advances in understanding the microbial processes involved,](#)  
870 [Environ. Microbiol. Rep., 1\(5\), 285–292, doi:10.1111/j.1758-2229.2009.00038.x, 2009.](#)

871 [Daims, H.: Use of fluorescence in situ hybridization and the daime image analysis program for the cultivation-](#)  
872 [independent quantification of microorganisms in environmental and medical samples, Cold Spring Harb. Protoc.,](#)  
873 [4\(7\), doi:10.1101/pdb.prot5253, 2009.](#)

874 [Dam, B., Dam, S., Kube, M., Reinhardt, R. and Liesack, W.: Complete genome sequence of Methylocystis sp.](#)  
875 [strain SC2, an aerobic methanotroph with high-affinity methane oxidation potential, J. Bacteriol., 194\(21\), 6008–](#)  
876 [6009, doi:10.1128/JB.01446-12, 2012.](#)

877 [DelSontro, T., Beaulieu, J. J. and Downing, J. A.: Greenhouse gas emissions from lakes and impoundments:](#)  
878 [Upscaling in the face of global change, Limnol. Oceanogr. Lett., 3\(3\), 64–75, doi:10.1002/lol2.10073, 2018.](#)

879 [Dumont, M. G., Pommerenke, B. and Casper, P.: Using stable isotope probing to obtain a targeted](#)  
880 [metatranscriptome of aerobic methanotrophs in lake sediment, Environ. Microbiol. Rep., 5\(5\), 757–764,](#)  
881 [doi:10.1111/1758-2229.12078, 2013.](#)

882 [Dunfield, P. F. and Conrad, R.: Starvation alters the apparent half-saturation constant for methane in the type II](#)  
883 [methanotroph Methylocystis strain LR1, Appl. Environ. Microbiol., 66\(9\), 4136–4138,](#)  
884 [doi:10.1128/AEM.66.9.4136-4138.2000, 2000.](#)

885 [Dunfield, P. F., Liesack, W., Henckel, T., Knowles, R. and Conrad, R.: High-affinity methane oxidation by a soil](#)  
886 [enrichment culture containing a type II methanotroph, Appl. Environ. Microbiol., 65\(3\), 1009–1014,](#)  
887 [doi:10.3109/17435390.2011.562327, 1999.](#)

888 [Eller, G., Stubner, S. and Frenzel, P.: Group-specific 16S rRNA targeted probes for the detection of type I and](#)  
889 [type II methanotrophs by fluorescence in situ hybridisation, FEMS Microbiol. Lett., 198\(2\), 91–97,](#)  
890 [doi:10.1016/S0378-1097\(01\)00130-6, 2001.](#)

891 [Graf, J. S., Mayr, M. J., Marchant, H. K., Tienken, D., Hach, P. F., Brand, A., Schubert, C. J., Kuypers, M. M. M.](#)  
892 [and Milucka, J.: Bloom of a denitrifying methanotroph, “Candidatus Methyloirabilis limnetica”, in a deep](#)  
893 [stratified lake, Environ. Microbiol., 20\(7\), 2598–2614, doi:10.1111/1462-2920.14285, 2018.](#)

894 [Guggenheim, C., Brand, A., Bürgmann, H., Sigg, L. and Wehrli, B.: Aerobic methane oxidation under copper](#)  
895 [scarcity in a stratified lake, Sci. Rep., 9\(1\), 1–11, doi:10.1038/s41598-019-40642-2, 2019.](#)

896 [Hanson, R. S. and Hanson, T. E.: Methanotrophic bacteria, Microbiol. Rev., 60\(2\), 439–471,](#)  
897 [doi:10.1002/0471263397.env316, 1996.](#)

898 [Hernandez, M. E., Beck, D. A. C., Lidstrom, M. E. and Chistoserdova, L.: Oxygen availability is a major factor](#)  
899 [in determining the composition of microbial communities involved in methane oxidation., PeerJ, 3\(e801\), 1–13,](#)  
900 [doi:10.7717/peerj.801, 2015.](#)

901 [Hyatt, D., Chen, G.-L., LoCascio, P. F., Land, M. L., Larimer, F. W. and Hauser, L. J.: Prodigal: prokaryotic](#)  
902 [gene recognition and translation initiation site identification, BMC Bioinformatics, 11\(119\), 1–11,](#)  
903 [doi:10.3389/fgene.2015.00348, 2010.](#)

904 [Kankaala, P., Taipale, S., Nykänen, H. and Jones, R. I.: Oxidation, efflux, and isotopic fractionation of methane](#)  
905 [during autumnal turnover in a polyhumic, boreal lake, J. Geophys. Res. Biogeosciences, 112\(2\), 1–7,](#)  
906 [doi:10.1029/2006JG000336, 2007.](#)

907 [Kirf, M. K., Dinkel, C., Schubert, C. J. and Wehrli, B.: Submicromolar oxygen profiles at the oxic-anoxic](#)  
908 [boundary of temperate lakes, Aquat. Geochemistry, 20\(1\), 39–57, doi:10.1007/s10498-013-9206-7, 2014.](#)

909 [Knief, C.: Diversity and habitat preferences of cultivated and uncultivated aerobic methanotrophic bacteria](#)  
910 [evaluated based on pmoA as molecular marker, Front. Microbiol., 6\(1364\), 1–38, doi:10.3389/fmicb.2015.01346,](#)  
911 [2015.](#)

912 [Knief, C. and Dunfield, P. F.: Response and adaptation of different methanotrophic bacteria to low methane](#)  
913 [mixing ratios, Environ. Microbiol., 7\(9\), 1307–1317, doi:10.1111/j.1462-2920.2005.00814.x, 2005.](#)

914 [Kojima, H., Iwata, T. and Fukui, M.: DNA-based analysis of planktonic methanotrophs in a stratified lake,](#)  
915 [Freshw. Biol., 54\(7\), 1501–1509, doi:10.1111/j.1365-2427.2009.02199.x, 2009.](#)

916 [Kolb, S., Knief, C., Dunfield, P. F. and Conrad, R.: Abundance and activity of uncultured methanotrophic](#)  
917 [bacteria involved in the consumption of atmospheric methane in two forest soils, Environ. Microbiol., 7\(8\),](#)  
918 [1150–1161, doi:10.1111/j.1462-2920.2005.00791.x, 2005.](#)

919 [Kopylova, E., Noé, L. and Touzet, H.: SortMeRNA: Fast and accurate filtering of ribosomal RNAs in](#)  
920 [metatranscriptomic data, Bioinformatics, 28\(24\), 3211–3217, doi:10.1093/bioinformatics/bts611, 2012.](#)

921 [Kuivila, K. M., Murray, J. W., Devol, A. H., Lidstrom, M. E. and Reimers, C. E.: Methane cycling in the](#)  
922 [sediments of Lake Washington, Limnol. Oceanogr., 33\(4\), 571–581, doi:10.4319/lo.1988.33.4.0571, 1988.](#)

923 [Kumar, S., Stecher, G. and Tamura, K.: MEGA7: Molecular evolutionary genetics analysis version 7.0 for bigger](#)  
924 [datasets, Mol. Biol. Evol., 33\(7\), 1870–1874, doi:10.1093/molbev/msw054, 2016.](#)

925 [Leak, D. J. and Dalton, H.: Growth yields of methanotrophs - 1. Effect of copper on the energetics of methane](#)  
926 [oxidation, Appl. Microbiol. Biotechnol., 23\(6\), 470–476, doi:10.1007/BF02346062, 1986.](#)

927 [Leys, C., Ley, C., Klein, O., Bernard, P. and Licata, L.: Detecting outliers: Do not use standard deviation around](#)  
928 [the mean, use absolute deviation around the median, J. Exp. Soc. Psychol., 49\(4\), 764–766,](#)  
929 [doi:10.1016/j.jesp.2013.03.013, 2013.](#)

930 [Li, D., Liu, C. M., Luo, R., Sadakane, K. and Lam, T. W.: MEGAHIT: An ultra-fast single-node solution for](#)  
931 [large and complex metagenomics assembly via succinct de Bruijn graph, Bioinformatics, 31\(10\), 1674–1676,](#)  
932 [doi:10.1093/bioinformatics/btv033, 2015.](#)

933 [Li, H., Handsaker, B., Wysoker, A., Fennell, T., Ruan, J., Homer, N., Marth, G., Abecasis, G. and Durbin, R.:](#)  
934 [The Sequence Alignment/Map format and SAMtools, Bioinformatics, 25\(16\), 2078–2079,](#)  
935 [doi:10.1093/bioinformatics/btp352, 2009.](#)

936 [Li, W. and Godzik, A.: Cd-hit: A fast program for clustering and comparing large sets of protein or nucleotide](#)  
937 [sequences, Bioinformatics, 22\(13\), 1658–1659, doi:10.1093/bioinformatics/btl158, 2006.](#)

938 [Liao, Y., Smyth, G. K. and Shi, W.: FeatureCounts: An efficient general purpose program for assigning sequence](#)  
939 [reads to genomic features, Bioinformatics, 30\(7\), 923–930, doi:10.1093/bioinformatics/btt656, 2014.](#)

940 [Liikanen, A., Huttunen, J. T., Valli, K. and Martikainen, P. J.: Methane cycling in the sediment and water column](#)  
941 [of mid-boreal hyper-eutrophic Lake Kevätön, Finland, Fundam. Appl. Limnol., 154\(4\), 585–603,](#)  
942 [doi:10.1127/archiv-hydrobiol/154/2002/585, 2002.](#)

943 [Lofton, D. D., Whalen, S. C. and Hershey, A. E.: Effect of temperature on methane dynamics and evaluation of](#)  
944 [methane oxidation kinetics in shallow Arctic Alaskan lakes, \*Hydrobiologia\*, 721\(1\), 209–222,](#)  
945 [doi:10.1007/s10750-013-1663-x, 2014.](#)

946 [Mayr, M. J., Zimmermann, M., Dey, J., Wehrli, B. and Bürgmann, H.: Data for: Community methane-oxidation](#)  
947 [kinetics selected by lake mixing regime \[Data set\], Eawag Swiss Fed. Inst. Aquat. Sci. Technol.,](#)  
948 [doi:10.25678/0001fa, 2019.](#)

949 [Mayr, M. J., Zimmermann, M., Guggenheim, C., Brand, A. and Bürgmann, H.: Niche partitioning of methane-](#)  
950 [oxidizing bacteria along the oxygen–methane counter gradient of stratified lakes, \*ISME J.\*, 14\(1\), 274–287,](#)  
951 [doi:10.1038/s41396-019-0515-8, 2020a.](#)

952 [Mayr, M. J., Zimmermann, M., Dey, J., Brand, A., Wehrli, B. and Bürgmann, H.: Growth and rapid succession of](#)  
953 [methanotrophs effectively limit methane release during lake overturn, \*Commun. Biol.\*, 3\(1\), 108,](#)  
954 [doi:10.1038/s42003-020-0838-z, 2020b.](#)

955 [O’Leary, N. A., Wright, M. W., Brister, J. R., Ciufu, S., Haddad, D., McVeigh, R., Rajput, B., Robbertse, B.,](#)  
956 [Smith-White, B., Ako-Adjei, D., Astashyn, A., Badretdin, A., Bao, Y., Blinkova, O., Brover, V., Chetvernin, V.,](#)  
957 [Choi, J., Cox, E., Ermolaeva, O., Farrell, C. M., Goldfarb, T., Gupta, T., Haft, D., Hatcher, E., Hlavina, W.,](#)  
958 [Joardar, V. S., Kodali, V. K., Li, W., Maglott, D., Masterson, P., McGarvey, K. M., Murphy, M. R., O’Neill, K.,](#)  
959 [Pujar, S., Rangwala, S. H., Rausch, D., Riddick, L. D., Schoch, C., Shkeda, A., Storz, S. S., Sun, H., Thibaud-](#)  
960 [Nissen, F., Tolstoy, I., Tully, R. E., Vatsan, A. R., Wallin, C., Webb, D., Wu, W., Landrum, M. J., Kimchi, A.,](#)  
961 [Tatusova, T., DiCuccio, M., Kitts, P., Murphy, T. D. and Pruitt, K. D.: Reference sequence \(RefSeq\) database at](#)  
962 [NCBI: Current status, taxonomic expansion, and functional annotation, \*Nucleic Acids Res.\*, 44\(D1\), D733–D745,](#)  
963 [doi:10.1093/nar/gkv1189, 2016.](#)

964 [Oksanen, J., Blanchet, F. G., Friendly, M., Kindt, R., Legendre, P., McGlenn, D., Minchin, P. R., O’Hara, R. B.,](#)  
965 [Simpson, G. L., Solymos, P., Stevens, M. H. H., Szoecs, E. and Wagner, H.: vegan: community ecology package](#)  
966 [2.5-6. \[online\] Available from: <https://cran.r-project.org/package=vegan>, 2019.](#)

967 [Oshkin, I. Y., Beck, D. A. C., Lamb, A. E., Tchesnokova, V., Benuska, G., Mctaggart, T. L., Kalyuzhnaya, M.](#)  
968 [G., Dedysh, S. N., Lidstrom, M. E. and Chistoserdova, L.: Methane-fed microbial microcosms show differential](#)  
969 [community dynamics and pinpoint taxa involved in communal response, \*ISME J.\*, 9\(5\), 1119–1129,](#)  
970 [doi:10.1038/ismej.2014.203, 2015.](#)

971 [Oswald, K., Milucka, J., Brand, A., Littmann, S., Wehrli, B., Kuypers, M. M. M. and Schubert, C. J.: Light-](#)  
972 [dependent aerobic methane oxidation reduces methane emissions from seasonally stratified lakes, \*PLoS One\*,](#)  
973 [10\(7\), 1–22, doi:10.1371/journal.pone.0132574, 2015.](#)

974 [Oswald, K., Graf, J. S., Littmann, S., Tienken, D., Brand, A., Wehrli, B., Albertsen, M., Daims, H., Wagner, M.,](#)  
975 [Kuypers, M. M. M., Schubert, C. J. and Milucka, J.: Crenothrix are major methane consumers in stratified lakes,](#)  
976 [\*ISME J.\*, 11\(9\), 2124–2140, doi:10.1038/ismej.2017.77, 2017.](#)

977 [Pernthaler, A., Pernthaler, J. and Amann, R.: Fluorescence in situ hybridization and catalyzed reporter deposition](#)  
978 [for the identification of marine bacteria, \*Appl. Environ. Microbiol.\*, 68\(6\), 3094–3101,](#)  
979 [doi:10.1128/AEM.68.6.3094, 2002.](#)

980 [R Core Team: A language and environment for statistical computing, 2018.](#)

981 [Remsen, C. C., Minnich, E. C., Stephens, R. S., Buchholz, L. and Lidstrom, M. E.: Methane oxidation in Lake](#)  
982 [Superior sediments, \*J. Great Lakes Res.\*, 15\(1\), 141–146, doi:10.1016/S0380-1330\(89\)71468-4, 1989.](#)

983 [Schmieder, R. and Edwards, R.: Quality control and preprocessing of metagenomic datasets, \*Bioinformatics\*,](#)  
984 [27\(6\), 863–864, doi:10.1093/bioinformatics/btr026, 2011.](#)

985 [Schubert, C. J., Diem, T. and Eugster, W.: Methane emissions from a small wind shielded lake determined by](#)  
986 [eddy covariance, flux chambers, anchored funnels, and boundary model calculations: A comparison, \*Environ.\*](#)  
987 [\*Sci. Technol.\*, 46\(8\), 4515–4522, doi:10.1021/es203465x, 2012.](#)

988 [Seemann, T.: Prokka: Rapid prokaryotic genome annotation, \*Bioinformatics\*, 30\(14\), 2068–2069,](#)  
989 [doi:10.1093/bioinformatics/btu153, 2014.](#)

990 [Semrau, J. D., DiSpirito, A. A., Gu, W. and Yoon, S.: Metals and methanotrophy, \*Appl. Environ. Microbiol.\*,](#)  
991 [84\(6\), 7–14, doi:10.1128/AEM.02289-17, 2018.](#)

992 [Shen, W., Le, S., Li, Y. and Hu, F.: SeqKit: A cross-platform and ultrafast toolkit for FASTA/Q file](#)  
993 [manipulation, \*PLoS One\*, 11\(10\), 1–10, doi:10.1371/journal.pone.0163962, 2016.](#)

994 [Steinle, L., Graves, C. A., Treude, T., Ferré, B., Biastoch, A., Bussmann, I., Berndt, C., Krastel, S., James, R. H.,](#)  
995 [Behrens, E., Böning, C. W., Greinert, J., Sapart, C. J., Scheinert, M., Sommer, S., Lehmann, M. F. and Niemann,](#)  
996 [H.: Water column methanotrophy controlled by a rapid oceanographic switch, \*Nat. Geosci.\*, 8\(5\), 378–382,](#)  
997 [doi:10.1038/ngeo2420, 2015.](#)

998 [Steinsberger, T., Schmid, M., Wüest, A., Schwefel, R., Wehrli, B. and Müller, B.: Organic carbon mass](#)  
999 [accumulation rate regulates the flux of reduced substances from the sediments of deep lakes, \*Biogeosciences\*,](#)  
1000 [14\(13\), 3275–3285, doi:10.5194/bg-14-3275-2017, 2017.](#)

1001 [Stuart, A. and Ord, J. K.: Kendall’s Advanced Theory of Statistics: Volume 1: Distribution Theory, Wiley., 2009.](#)

1002 [Sundh, I., Bastviken, D. and Tranvik, L. J.: Abundance, activity, and community structure of pelagic methane-](#)  
1003 [oxidizing bacteria in temperate lakes, \*Appl. Environ. Microbiol.\*, 71\(11\), 6746–6752,](#)  
1004 [doi:10.1128/AEM.71.11.6746-6752.2005, 2005.](#)

1005 [Taubert, M., Grob, C., Crombie, A., Howat, A. M., Burns, O. J., Weber, M., Lott, C., Kaster, A. K., Vollmers, J.,](#)  
1006 [Jehlich, N., von Bergen, M., Chen, Y. and Murrell, J. C.: Communal metabolism by \*Methylococcaceae\* and](#)  
1007 [\*Methylophilaceae\* is driving rapid aerobic methane oxidation in sediments of a shallow seep near Elba, Italy,](#)  
1008 [\*Environ. Microbiol.\*, 21\(10\), 3780–3795, doi:10.1111/1462-2920.14728, 2019.](#)

1009 [Trotsenko, Y. A. and Khmelena, V. N.: Aerobic methanotrophic bacteria of cold ecosystems, \*FEMS Microbiol.\*](#)  
1010 [\*Ecol.\*, 53\(1\), 15–26, doi:10.1016/j.femsec.2005.02.010, 2005.](#)

1011 [Tveit, A. T., Hestnes, A. G., Robinson, S. L., Schintlmeister, A., Dedysh, S. N., Jehlich, N., Von Bergen, M.,](#)  
1012 [Herbold, C., Wagner, M., Richter, A. and Svenning, M. M.: Widespread soil bacterium that oxidizes atmospheric](#)  
1013 [methane, \*Proc. Natl. Acad. Sci. U. S. A.\*, 116\(17\), 8515–8524, doi:10.1073/pnas.1817812116, 2019.](#)

1014 [Wagner, G. P., Kin, K. and Lynch, V. J.: Measurement of mRNA abundance using RNA-seq data: RPKM](#)  
1015 [measure is inconsistent among samples, \*Theory Biosci.\*, 131\(4\), 281–285, doi:10.1007/s12064-012-0162-3, 2012.](#)

1016 [Wiesenburg, D. A. and Guinasso, N. L.: Equilibrium solubilities of methane, carbon monoxide, and hydrogen in](#)  
1017 [water and sea water, \*J. Chem. Eng. Data\*, 24\(4\), 356–360, doi:10.1021/jc60083a006, 1979.](#)

1018 [Zimmermann, M., Mayr, M. J., Bouffard, D., Eugster, W., Steinsberger, T., Wehrli, B., Brand, A. and Bürgmann,](#)  
1019 [H.: Lake overturn as a key driver for methane oxidation, \*bioRxiv\*, doi:10.1101/689182, 2019.](#)